UC Santa Cruz

UC Santa Cruz Electronic Theses and Dissertations

Title

The Collaborative Regulation of Cortical Neuron Subtype Specification by TLE4 and FEZF2

Permalink

https://escholarship.org/uc/item/8dc445dc

Author

Tastad, David John

Publication Date

2020

Peer reviewed|Thesis/dissertation

eScholarship.org Powered by the California Digital Library
University of California

UNIVERSITY OF CALIFORNIA
SANTA CRUZ

THE COLLABORATIVE REGULATION OF CORTICAL NEURON SUBTYPE SPECIFICATION BY *TLE4* AND *FEZF2*

A dissertation submitted in partial
satisfaction of the requirements for the
degree of

DOCTOR OF PHILOSOPHY

in

MOLECULAR, CELL, AND DEVELOPMENTAL BIOLOGY

by

David J. Tastad

March 2020

The Dissertation of David J. Tastad is approved:

Professor Bin Chen, chair

Professor David Feldheim

Professor James Ackman

Quentin Williams
Acting Vice Provost and Dean of Graduate Studies

Copyright © by
David J. Tastad
2020

Table of Contents

List of Figures

Chapter 1:

Chapter 2:

Abstract

THE COLLABORATIVE REGULATION OF CORTICAL NEURON SUBTYPE SPECIFICATION BY *TLE4* AND *FEZF2*

David J. Tastad

Projection neuron subtype identities in the cerebral cortex are established through the expression of pan-cortical and subtype-specific effector genes, which execute terminal differentiation programs that bestow neurons with a glutamatergic neuron phenotype and subtype-specific morphology, physiology, and axonal projections. Whether pan-cortical glutamatergic and subtype-specific characteristics are regulated by the same genes or controlled by distinct programs remains largely unknown. Here, I show that the transcriptional corepressor, TLE4, is expressed specifically in postmitotic corticothalamic projection neurons, where it functions to regulate the molecular, dendritic, and electrophysiological characteristics unique to corticothalamic neurons. I also demonstrate that TLE4 directly interacts with the forebrain embryonic zinc finger protein, FEZF2, within corticothalamic projection neurons to facilitate the transcriptional repression of subcerebral projection neuron identity. Through the utilization of our novel *Fezf2-Bac-EnR* transgenic mouse line, I was then

able rescue the molecular defects of corticothalamic neurons in the cortex of *Tle4* knockout mice and restore the dendritic and electrophysiological characteristics of theses neurons. Overall, the work presented provides an in-depth investigation into the transcriptional regulation of subtype-specific cortical projection neuron identity by *Tle4* and *Fezf2*, thereby contributing novel insight into our current understanding of mammalian cortical development.

Acknowledgments

First and foremost, I would like to express my deepest gratitude to my advisor, Dr. Bin Chen, for your constant guidance throughout the PhD program. Your genuine passion and commitment to your research has deeply inspired me from the day I joined your lab. I would not be who I am today without all of your constructive criticism, guidance, and support. You have truly shaped me into what I believe to be a well-rounded, honest, and dedicated scientist, and I appreciate this immensely.

I would also like to thank Professors David Feldheim, and James Ackman for their thoughtful advice and constructive criticism during my oral examination, as well as their support and assistance on my thesis research. Dave, it has truly been a pleasure working with you on the third floor, and I will miss our occasional chats in the hallway, as they were always a pleasant relief from work. Also, the MCD biology retreats would never have been as fun for me without you two being there. Again, thank you for all of the intellectual and moral support throughout the years.

Importantly, I would like to thank all current and past members of the Chen lab, for their thoughtful input into my dissertation research. You are all some of my best friends, and the work I have performed in this lab could never have been possible without your help. In particular, I am deeply grateful for Christian Ortiz initially accepting me into the lab, where he showed

exceptional levels of patience and support, ultimately allowing me flourish as a scientist. You taught me nearly all of the techniques that I have now begun to master, and it would have never been possible without you.

Jeremiah Tsyporin, we have had some great times together the last 5-6 years of our lives, and this program would not have been nearly as fun or productive without you. As you know, working together on this project had its ups and downs, but I want to say that I genuinely admire what we have accomplished together, and what you will undoubtedly accomplish in the future. The following graduate students in the Chen lab have all played particularly essential roles in the work presented here: Jeremiah Tsyporin, Kendy Hoang, Liora Huebner, and Tommy Finn. This work research would not have been possible without all of your help.

Additionally, I would like to thank Dr. John Rubenstein, Dr. Susan McConnell, Dr. Nenad Sestan, and Dr. Shenfeng Qiu, for their helpful comments into the dissertation work herein, as well as previous projects.

I can’t emphasize enough how thankful I am for the love and support my family has always shown. Mom, Dad, Blake, and Johnny, I love you all so much, and I am so incredibly grateful for all of your encouragement throughout this lengthy endeavor. I am blessed to have you all by my side.

This work was supported by the research grant R01MH09458907. The findings presented here represent a substantial collaborative effort, which

would have otherwise been impossible to accomplish without the fantastic group of friends, family, coworkers, collaborators, and advisors I have just described.

Chapter 1: Introduction

The human cerebral cortex is comprised of six distinct layers and contains roughly 50 to 65 billion neural and glial cells (Pelvig et al., 2007). It is responsible for cognition, perception, and complex behaviors unique to humans. The coordinated generation of diverse cortical neuron subtypes, and their wiring into functional neural circuits is fundamental for its proper function. Both intrinsic (e.g., transcription factor-mediated gene regulation) and extrinsic (e.g., environmental and extracellular signals) cues delicately orchestrate these complex tasks throughout development. Indeed, mutations in genes regulating cortical neuron fate specification and differentiation have been identified as causes for neurodevelopmental disorders such as intellectual deficiency and autism, and these genes are conserved in mice (Balasubramanian et al., 2011; Docker et al., 2013; Willsey et al., 2013; Notwell et al., 2016). Studying these genes in mice allows for genetic gain and loss-of-function studies that have proven instrumental in gaining a deeper understanding of mammalian cortical development. Although we and others have begun to elucidate key transcriptional regulators directly involved in the terminal differentiation and subtype specification of cortical projection neurons, the molecular logic for this remains largely unknown.

Radial Glial Cells of the Cerebral Cortex

Embryonic neural progenitor cells (NPCs) were initially described in the 19th century by Dr. Golgi and Dr. Ramón y Cajal and are now known to be the progenitor cells that give rise to the neurons and glia that make up the mammalian central nervous system. The NPCs of the developing cerebral cortex have long been studied and were termed radial glial cells (RGCs) in 1971 by Dr. Pasko Rakic, reflecting their radial orientation in the developing telencephalon and their non-mature glial cell-like morphology (Rakic 1971a; Rakic 1972). RGCs occupy the cortical ventricular zone (VZ), where they are structurally and genetically primed to produce excitatory glutamatergic projection neurons in early development, and then produce astrocytes and oligodendrocytes later in development (Figure 1-1). Initially, early NPCs in the VZ undergo multiple rounds of symmetric cell divisions; this expands the overall RGC population (Figure 1-1). RGCs will then divide asymmetrically to produce one intermediate progenitor cell (IPC) which will occupy the subventricular zone (SVZ), and one RGC that will remain in the VZ (Figure 1-1). The IPC will ultimately divide and terminally differentiate into multiple types of excitatory projection neurons that will migrate into the developing cortical plate of the neocortex. (Figure 1-1). Thus, RGCs must maintain an intricate balance between proliferation and differentiation to generate the correct number of projection neurons and glial cells.

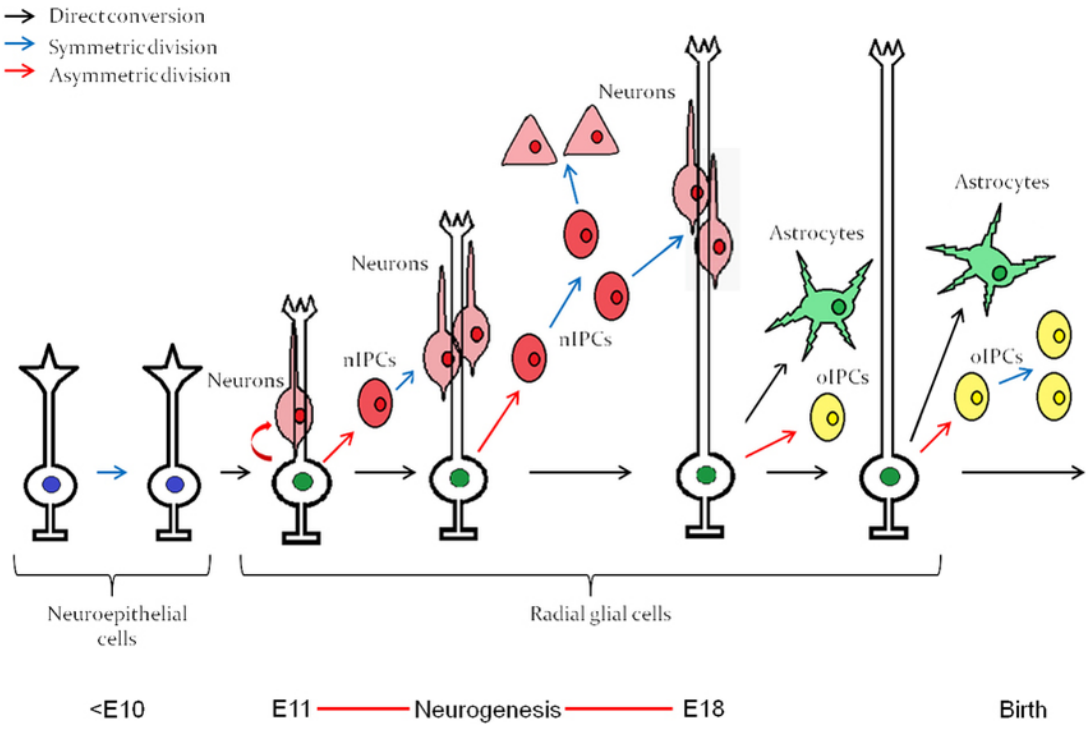

Figure 1-1: Schematic of embryonic neuro- and gliogenesis of the cortex. Embryonic neuroepithelial (NE) cells of the neural tube give rise to radial glial cells, which first differentiate into neurons and then into astrocytes. The neurogenesis "window" extends approximately from E11 to E18. nIPC, neurogenic intermediate progenitor cell; oIPC, oligodendrogenic intermediate progenitor cell. This figure is representative of embryonic neurogenesis in the mouse. (Kriegstein & Alvarez-Buylla, 2009).

RGC's have a unique structure, unlike most neurons they extend two processes from their cell bodies, one long basal process which reaches the pial surface and one much shorter apical process that descends to the ventricular surface. This distinct morphological characteristic of RGCs is fundamental to the proper development of the cerebral cortex. The central role of the apical process is to regulate the balance between proliferation and differentiation. Multiple studies have begun to uncover the critical

mechanisms involved in this process, such as integrin/laminin mediated end-feet binding to the ventricular surface, Eph/ephrin signaling cascades localized at the apical process, and apical protocadherin adhesive complexes (Kadowaki et al., 2007; Nievergall et al., 2012; Ishiuchi et al., 2009). Indeed, mutations of proteins in these structures and pathways affect the regulation of proliferation versus differentiation and have been implicated in diseases such as heterotopias, microcephaly, and macrocephaly (Schmid et al., 2014; Bizzotto and Francis 2015).

The basal processes of RGCs, however, serve a vastly different role in cortical development. The basal process constitutes a scaffold for which newly born neurons will use to migrate through the SVZ and previously formed cortical layers until they reach their final position within the cortical plate (Figure 1-1). The absence or perturbation of this basal process causes severe defects in neuronal migration, ultimately leading to vast cortical malformation (Bizzotto and Francis 2015).

In addition to the overall structure of RGCs, the tight regulation of target-gene expression by transcription factors in RGCs is essential for the generation and organization of glutamatergic projection neurons in the cortex (Konno et al., 2019; Desmaris et al., 2018; Kroll et al., 2005; Schuurmans et al., 2004). Early in cortical developmental, the transcription factor *Sox2*, among others, maintain precursor identity by inhibiting their differentiation, thereby expanding the progenitor population (Graham et al., 2003; Mitzutani

et al., 2007; Martynoga et al., 2012). As development proceeds, transcription factors expressed in cortical RGCs and/or intermediate progenitors (including *Pax6*, *Tlx*, *Dmrt5*, *Dmrt3*, *Emx2*, *Ngn1*, and *Ngn2*) actively promote the generation of cortical glutamatergic projection neurons and prevent the production of ventral GABAergic neurons (Konno et al., 2019; Desmaris et al., 2018; Kroll et al., 2005; Schuurmans et al., 2004). Despite many fundamental advances in this field, our understanding of the spatial, temporal, and cell type-specific mechanisms of these key factors remains incomplete.

Projection Neuron Subtype Specification

As mentioned earlier, RGCs in the cortical VZ give rise to transient intermediate progenitor cells (IPCs), which reside in the SVZ until they differentiate into specific cortical projection neurons. Broadly, excitatory projection neurons of the mammalian cerebral cortex can be classified into 3 major subtypes based on where they project their axons. Corticocortical neurons project axons to the ipsilateral (intracortical) or contralateral (callosal) cortex and are found in layers 2 through 6. Corticothalamic neurons reside in layer 6 and extend axons into the thalamus. They are essential in sensory processing, and their dysfunction has been implicated in epilepsy (Mattson, 2003). Subcerebral neurons project axons into the midbrain, hindbrain, and spinal cord, and are confined to layer 5 (O'Leary and Koester, 1993). This subtype includes corticospinal motor neurons, which are clinically important

neurons that degenerate in Amyotrophic Lateral Sclerosis and are damaged in spinal cord injury (Grosskreutz et al., 2006; Habert et al., 2007).

The development of distinct cortical projection neuron subtypes relies heavily on a network of transcription factors that mostly act by cross inhibiting the expression of each other. For example, the zinc-finger transcription factor, *Fezf2*, is expressed in deep-layer neurons (layers 5 and 6) and is the major cell fate-determining gene for subcerebral neurons. FEZF2 represses high-level expression of *Tbr1* and *Satb2* in deep layer neurons, thereby preventing alternate corticothalamic and callosal identities (Arlotta et al., 2005; Chen et al., 2005a; Chen et al., 2008; Chen et al., 2005b; Molyneaux et al., 2005). Additionally, TBR1 and SOX5 directly repress high levels of *Fezf2* expression in layer 6 neurons, thereby repressing subcerebral neuron identity and driving corticothalamic neuronal fate (Kwan et al., 2008; Lai et al., 2008; McKenna et al., 2011; Han et al., 2011). Another example of transcriptional repression of alternative identities is the role of transcription factor SATB2, which is specifically expressed in callosal neurons and promote callosal neuron identity by repressing genes that are essential for subcerebral axon development (Alcamo et al., 2008; Britanova et al., 2008).

Despite this exciting progresses, recent studies suggest that our current understanding of the molecular mechanism for cortical projection neuron fate specification and differentiation is incomplete and somewhat incorrect. For example, while SATB2 was initially reported to promote callosal

neuron identity by repressing expression of genes essential for subcerebral axon development (Alcamo et al., 2008; Britanova et al., 2008), it was recently shown that SATB2 is also expressed in subcerebral neurons and is essential for their fate specification (McKenna et al., 2015). Similarly, although *Sox5* was reported to promote corticothalamic neuron fate by directly repressing *Fezf2* expression (Kwan et al., 2008), it has since been found that subcerebral neurons and axons are completely missing in *Sox5* mutant brains (McKenna et al., 2015). Therefore, we must continuously question and investigate the intricate mechanisms underlying neuronal fate specification.

The FEZ and TLE protein families

Transcription factors typically function to either promote or suppress the expression of a specific set of target genes, however some transcription factors have been shown to do both depending on the context. Most transcription factors have DNA-binding domains which will bind either one particular DNA sequence, or a slightly variable DNA motif in the genome to exert transcriptional regulation. Interestingly, it is not the case that all transcriptional regulators bind to DNA directly. Thus, they are termed transcriptional coactivators or corepressors.

Coactivators increase transcription levels primarily by connecting DNA-binding transcription factors to general transcription machinery and navigating these activators through the constraints of chromatin to their target gene

(Naar et al., 2001). Corepressors function primarily either through the short-range quenching of transcriptional activation near the promotor region of genes, or through long-range mechanisms by interacting with chromatin remodeling machinery to elicit widespread chromatin remodeling thereby generating a repressed chromosomal state (Li and Arnosti, 2011; Chen and Courey, 2000; Liu and Karmarkar, 2008). Just as transcriptional activators and repressors contain highly conserved DNA binding domains to guide them to their target sequences, transcriptional coactivators and corepressors contain highly conserved domains which direct them to bind other specific proteins.

The *Drosophila* Groucho (Gro) protein is the prototype for a large family of corepressors that are involved in many developmental processes. One group within this family is the Transducin-like Enhancer of split (*Tle*) corepressors, which are the mammalian homologues of the Groucho related genes (*Grg*) initially described in *Drosophila* (Chen et al., 2000). The *Tle* family consists of four transcriptional corepressors (*Tle1, Tle2, Tle3,* and *Tle4*) and do not bind to DNA directly, but rather are recruited to DNA-bound proteins to repress gene expression and are therefore referred to as transcriptional corepressors (Chen et al., 2000). *Tle* family members are required for many developmental processes, including lateral inhibition, segmentation, sex determination, dorsal/ventral pattern formation, terminal pattern formation, and eye development (Chen et al., 2000). All four members

of the *Tle* family contain the highly conserved WD40 repeat domain. This domain directly promotes the binding of TLE proteins to transcription factors containing an Eh1 or WRPW domain (Courey and Jia, 2001; Smith and Jaynes, 1996; Jimenez et al., 1997; Tolkunova et al., 1998).

The forebrain embryonic zinc finger (FEZ) family is a highly conserved family of transcription factors initially discovered in the anterior neuroepithelium of *Xenopus* and zebrafish embryos (Shimizu and Hibi, 2009). The vertebrate FEZ family contains two members, *Fezf1* and *Fezf2*. Both proteins express six C2H2 Zinc-finger domains and an Engrailed homology 1 (Eh1) domain. The Zinc-finger domain is a well characterized protein domain involved in the direct binding of DNA and was originally characterized in 1987 by Aaron Klug (Klug and Rhodes 1987). Additionally, Eh1 domains are now known to directly interact with the Groucho/TLE family of transcriptional corepressors, leading to transcriptional repression (Hashimoto et al., 2000b).

Innovation and Significance

The research presented here investigates the role of the transcriptional co-repressor, *Tle4*, and the transcription factor *Fezf2*, in cortical neuron subtype specification. Previously, TLE4 has been assumed to be a marker for CThPNs based solely on its specific layer 6 expression pattern, but this assumption has never been confirmed in a quantitative manner. Additionally,

the function of TLE4 in cortical neuron fate specification has never been investigated. In this dissertation, I first show quantitatively that TLE4 is highly specific to CThPNs through the injection of retrograde tracers into various brain regions. Upon confirming the high corticothalamic specificity of TLE4, I began to investigate the potential role of TLE4 in the generation, refinement, or maintenance of corticothalamic neurons. Through the use of our novel transgenic *Tle4* knockout mouse line, I was able to meticulously investigate the various roles of TLE4 in corticothalamic neurons. I found that TLE4 functions to regulate the molecular identity, dendritic morphology, and electrophysiological properties of corticothalamic projection neurons. The research presented here also clarifies a few key misconceptions regarding our current understanding of cortical neuron subtype specification. Specifically, others have assumed that FEZF2 expression is restricted to subcerebral neurons, but here I show that in layer 6 corticothalamic neurons, TLE4 directly interacts with FEZF2 to inhibit the expression of genes associated with subcerebral neuron identity, to guide the molecular refinement of corticothalamic neurons.

Having a complete understanding of how different cortical projection neurons are generated and subsequently wire together to form complex functional neural circuits during development will not only provide deep insight into the mechanisms of human brain development, but also will reveal the biological causes of various developmental and cognitive brain disorders,

such as ALS, mental retardation, schizophrenia, and autism. Thus, the results from my dissertation research will have fundamental importance in developmental biology, stem cell biology, human disease mechanisms, and their potential therapies. The text of this dissertation will present, discuss, and interpret results from the following research manuscript currently in submission for publication:

Tastad D and Tsyporin J, Ma X, Nehme A, Finn T, Huebner L, Liu G, Makhamreh A, Gallardo D, Roberts JM, Katzman S, Sestan N, McConnell SK, Yang Z, Qiu S, Chen B (2020). Transcriptional repression by FEZF2 restricts alternative identities of cortical projection neurons.

Chapter 2: Transcriptional regulation of subtype-specific projection neuron identities in the developing cerebral cortex by FEZF2 and TLE4

Introduction

Projection neuron subtype identities in the developing cerebral cortex are established through the expression of pan-cortical and subtype-specific genes, which execute terminal differentiation programs and bestow neurons with a glutamatergic phenotype and subtype-specific morphology, physiology, and axonal projections. Whether the pan-cortical glutamatergic phenotype and subtype-specific characters are regulated by the same genetic program or controlled by distinct genes remains largely unknown. In *C. elegans*, expression of terminal effector genes is activated by terminal selector genes, which are transcription factors that act in differentiating neurons by binding to common cis-regulatory elements in effector genes and activating their expression (Hobert & Kratsios 2019). Whether similar mechanisms are utilized in developing mammalian brains is unknown, with the exception of the corticospinal neurons (CSNs), a subset of subcerebral projection neurons that are specified by the transcriptional regulator FEZF2 (Lodato et al.,2014).

Although recent advances in single-cell RNA-sequencing (scRNA-seq) technologies have allowed classification of neurons into different clusters

based on gene expression in individual cells (Tasic et al., 2018), neocortical excitatory neurons can be broadly classified into 3 major subtypes based on where they project axons (Leone et al., 2008). Corticocortical neurons, located in layers 2-6, project axons to the ipsilateral (intracortical) or contralateral (callosal) cortex. The subcerebral neurons projecting to the thalamus (corticothalamic neurons), mostly reside in layer 6, whereas the subcerebral neurons projecting to the midbrain, hindbrain, and spinal cord are confined to layer 5B (O'Leary & Koester 1993). Determining the molecular mechanisms underlying the differentiation of these neuronal subtypes is essential for understanding the regulatory logic of cell fate specification in the neocortex.

Prior studies have identified several genes that broadly specify the identities of cortical projection neuron subtypes and revealed that the development of these subtypes depends on a network of transcription factors that cross-inhibit one another's expression. The zinc-finger transcription factor *Fezf2* is expressed in deep-layer neurons. It promotes a subcerebral neuronal identity and suppresses expression of subtype-determining genes for corticothalamic (*Tbr1*) and callosal (*Satb2*) neurons (Chen et al., 2005; Chen et al., 2008; Chen J et al., 2005; Molyneaux et al., 2005). *Bcl11b*, also known as *Ctip2*, encodes a zinc-finger transcription factor expressed at high levels in layer 5 subcerebral neurons and at low levels in layer 6 corticothalamic neurons (McKenna et al., 2011). It regulates extension and fasciculation of

subcerebral axons (Arlotta et al., 2005). *Tbr1* and *Sox5* are both expressed at high levels in corticothalamic projection neurons. They promote a corticothalamic neuronal fate and directly repress *Fezf2* expression and subcerebral identity in layer 6 neurons (McKenna et al., 2011; Lai et al., 2008; Han et al., 2011; Kwan et el., 2008). *Satb2* was initially reported to be specifically expressed in callosal neurons, where it promotes a callosal neuron identity by repressing genes including *Bcl11b* that are essential for subcerebral axon development (Alcamo et al., 2008; Britanova et al., 2008). Recent studies show *Satb2* is also expressed in subcerebral neurons and is required for their fate specification (Leone et al., 2015; McKenna et al., 2015).

Despite the identification of these critical transcription factors, the molecular logic for cortical neuron subtype specification remains elusive. *Fezf2* has been the prototypic transcription factor for studying this process in subcerebral neurons. A recent study reported that *Fezf2* directly activates the expression of genes conferring glutamatergic and subcerebral neuronal identity, and represses genes associated with GABAergic and callosal neuron phenotypes, suggesting that, similar to *C. elegans* neurons (Hobert & Kratsios 2019), the subtype identities of cortical excitatory neurons are specified by terminal selector genes (Lodato et al., 2014). However, the ability of *Fezf2* to directly activate the expression of terminal effector genes has not been rigorously tested. *Fezf2* is expressed in both radial glial cells (RGCs) and in postmitotic neurons (Chen et al., 2005; Chen et al., 2008; Chen J et al., 2005;

Molyneaux et al., 2005; Guo et al., 2013), and it is unclear whether *Fezf2* is required in RGCs or in newly-generated neurons to specify a subcerebral neuronal fate. The N-terminal of FEZF2 protein contains an Engrailed Homology domain (EH1), which is known to recruit the Transducin-Like Enhancer of Split (TLE) family transcriptional co-repressors (Hashimoto et al., 2000). It remains to be determined if FEZF2 functions as a transcriptional repressor, an activator, or both, during cortical development. Finally, previous studies and recent scRNA-seq analyses revealed that, in addition to subcerebral neurons, *Fezf2* is expressed in corticothalamic and deep-layer callosal neurons (Tasic et al., 2018; Molyneaux et al., 2007; Clare et al., 2017; Tantrigama et al., 2016). If *Fezf2* is the terminal selector gene for subcerebral neurons, what is the function of *Fezf2* in these other cell types?

Here we address these questions and demonstrate that *Fezf2* functions as a selective repressor in multiple neuronal subtypes to repress the expression of genes associated with alternate subtypes. We show that in CThPNs, FEZF2 and TLE4 co-regulate the molecular differentiation, dendritic morphology, and function of these neurons. Together with previous studies, our results suggest that distinct genetic programs act sequentially to regulate the differentiation of projection neurons, with genes expressed in progenitor cells specifying the pan-cortical glutamatergic phenotype, and subtype-specifying transcription factors functioning in postmitotic cells to selectively repress the expression of genes associated with alternate subtype identities.

Results

Fezf2 is required in postmitotic neurons to regulate the development of both subcerebral and corticothalamic identities

To determine whether *Fezf2* acts in cortical RGCs or in postmitotic neurons to specify projection neuron subtype identities, we generated *Fezf2* conditional knockout mice (*Fezf2 cko*) using a $Fezf2^{Flox}$ allele (Shim et al., 2012) and the Nex^{Cre} allele (Goebbels et al., 2006) to delete *Fezf2* in postmitotic neurons. Western blot analysis using a C-terminal FEZF2 antibody revealed that while FEZF2 protein was absent in the $Fezf2^{-/-}$ null mutant cortices, a faint band of full-length FEZF2 was detected in the Nex^{Cre} $Fezf2^{Flox/-}$ (*Fezf2 cko*) cortices, indicating that the recombination was incomplete (Figures 1a and 2b). In addition, a smaller 20 kDa band was detected in *Fezf2 cko* cortices, corresponding to the truncated C-terminal half and DNA binding domain of FEZF2 (Figure 1a and Supplementary Figure 1a-b).

We compared cortices from *Fezf2 cko* mice to $Fezf2^{+/-}$ and $Fezf2^{-/-}$ cortices at P0 and P7 (Figures 1b-d and Supplemental Figure 1). The $Fezf2^{-}$ null mutant allele contained a *PLAP* (human placenta alkaline phosphatase) knock-in gene under the control of endogenous *Fezf2* promoter, and enabled us to directly observe the axons from *Fezf2*-expressing neurons (Chen et al.,2015). The phenotypes of *Fezf2 cko* and $Fezf2^{-/-}$ cortices were similar: (1)

the expression of subcerebral neuronal genes including BCL11B and BHLHB5 was significantly reduced in layer 5 neurons (Figure 1b,c); (2) expression of corticothalamic neuron genes such as TBR1 and genes expressed at high levels in the callosal neurons such as SATB2 was increased in layer 5 (Supplemental Figure 1c-d), suggesting that subcerebral neurons adopted corticothalamic and callosal identities; (3) expression of corticothalamic neuronal genes such as TLE4, ZFPM2 (FOG2) and FOXP2 was decreased in layer 6 neurons (Figure 1b-c, Supplemental Figure 1e-f); (4) expression of BCL11B was increased in layer 6, demonstrating that the molecular distinction between subcerebral and corticothalamic neurons failed to be refined in these cells (Figure 1b-c, Supplemental Figure 1b, 1e-f); (5) $PLAP^+$ subcerebral axons were significantly reduced in the pyramidal decussation (Figure 1d); and (6) consistent with a previous report (Diao et al., 2018), $PLAP^+$ corticothalamic axons to the dLGN and other thalamic nuclei were severely reduced in both *Fezf2 cko* and *Fezf2*$^{-/-}$ mice (Figure 1d).

Despite these similarities, the phenotypes of *Fezf2 cko* and *Fezf2*$^{-/-}$ cortices were not identical, likely due to incomplete recombination in *Fezf2 cko* mice (Figure 1a). Specifically, *Fezf2 cko* cortices contained a few $BCL11B^+BHLHB5^+$ subcerebral neurons (Figure 1b-c) and some $PLAP^+$ corticospinal axons were able to project to the pyramidal decussation (Figure 1d). However, the similarity between the phenotypes of *Fezf2 cko* and *Fezf2*$^{-/-}$ mice indicates that *Fezf2* is required in postmitotic neurons to regulate the

molecular identities and axonal projections of both subcerebral and corticothalamic neurons.

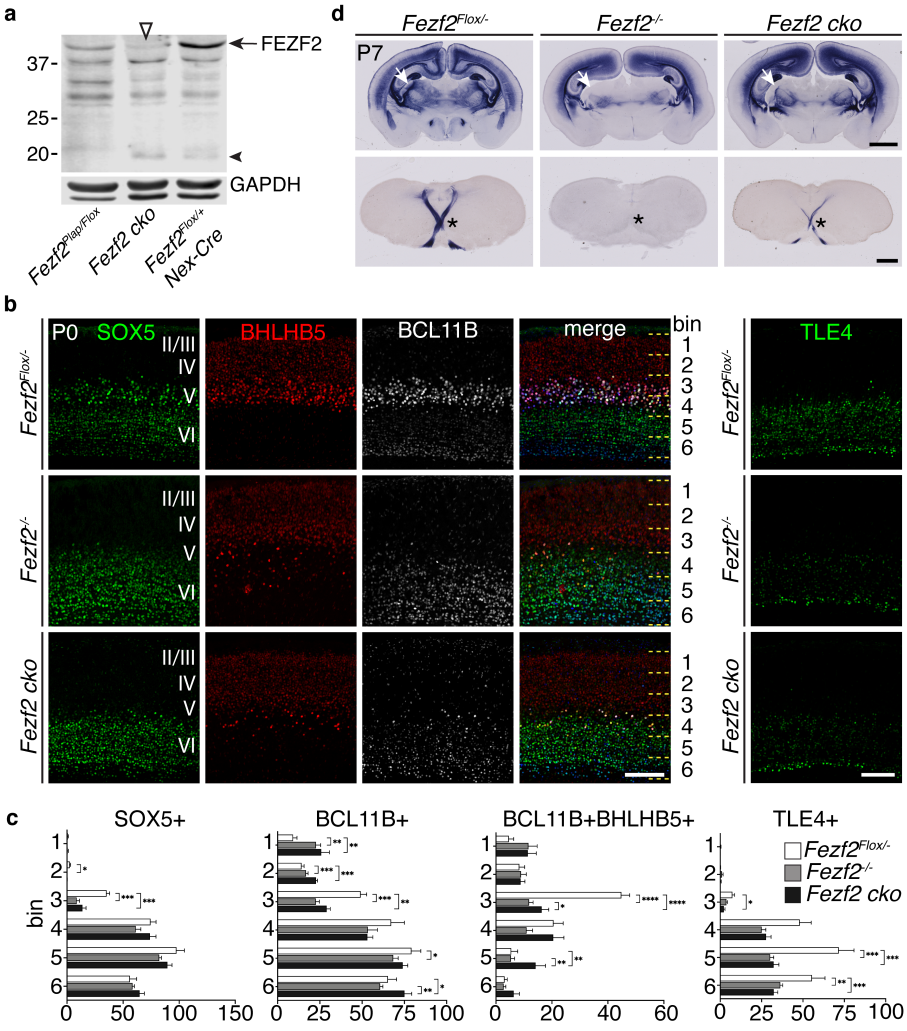

Figure 1: *Fezf2* functions in postmitotic neurons to specify cell identity.
a. Western Blot showing a reduction of full-length FEZF2 protein (arrow) in the *Fezf2 cko* cortices. Empty triangle points to residual FEZF2 protein in the *Fezf2 cko* cortices. Recombined *Fezf2^{flox}* allele produced a truncated FEZF2 (arrowhead) corresponding to the C-terminal half of the protein (see Fig S1a). **b-c**. Immunostains for SOX5, BHLHB5, BCL11B, and TLE4 on sections from P0 *Fezf2$^{+/-}$*, *Fezf2$^{-/-}$*, and *Fezf2 cko* mice. Cortices were divided into 6 equal bins and the numbers of cells in each bin were counted. Scale bars:100 µm. **d**. Quantifications for marker^{+} neurons per 10,000 µm^2 in each bin(width:250µm). n=3 brains/genotype, 3 sections/brain. Error bars represent ± SEM. Statistical significance was determined using one-way ANOVA followed by Tukey's t-test (*p<0.05, **p<0.01, ***p<0.001, ****p<0.0001). **d**. PLAP staining of brain sections of P7 *Fezf2$^{-/Flox}$*, *Fezf2$^{-/-}$*, and *Fezf2 cko* mice. The top row shows coronal cortical sections, the bottom row shows coronal sections at the level of pyramidal decussation. White arrows: dLGN; *: pyramidal decussation. Scale bars: top: 1 mm. bottom: 500 µm.

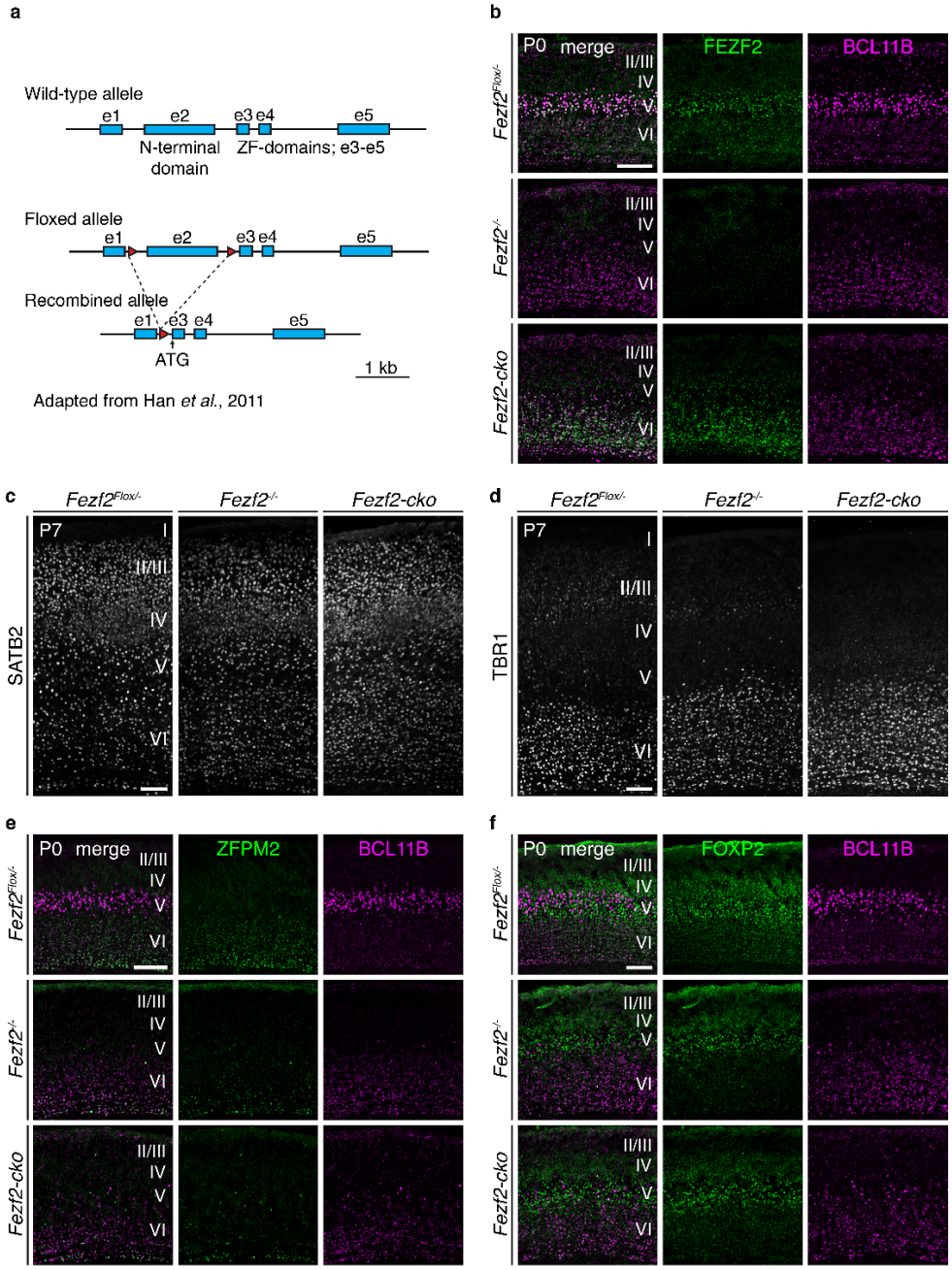

Figure S1. The *Fezf2*$^{-/-}$ and *Fezf2 cko* mice show similar molecular defects in the cortical projection neurons.

a. Recombined *Fezf2*^{Flox} allele encodes a truncated FEZF2 protein containing the zinc finger DNA binding domain alone **b**. Staining using C-terminal FEZF2 antibody shows the complete absence of FEZF2 protein in *Fezf2*$^{-/-}$ mice, and increased expression of truncated FEZF2 in layer 6 in *Fezf2 cko* mice. **c**. SATB2 expression is

increased in deep layers of *Fezf2*$^{-/-}$ and *Fezf2 cko* cortices. **d**. TBR1 is increased in layer 5 of *Fezf2*$^{-/-}$ and *Fezf2 cko* cortices. **e-f**. ZFPM2 (**e**) and FOXP2 (**f**) expression is reduced in layer 6 of *Fezf2*$^{-/-}$ and *Fezf2 cko* cortices. Scale bars: 100 μm.

FEZF2 functions as a transcriptional repressor to specify cortical projection neuron subtypes

FEZF2 protein consists of an N-terminal half containing an EH1 domain and other sequences, and a C-terminal half consisting of six C2H2-type zinc-finger motifs (Hashimoto et al., 2000). Zinc finger motifs are involved in DNA binding, and the EH1 domain recruits the TLE family transcriptional co-repressors. To test whether FEFZ2 functions as a transcriptional repressor, an activator, or both, we generated expression plasmids encoding a full-length FEZF2 protein, a chimeric protein consisting of the transcriptional repressor domain of the engrailed protein (EnR) fused with the DNA-binding domain of FEZF2 (*pCAG-Fezf2-EnR*), or a chimeric protein consisting of the VP16 transcription activator domain (VP16) fused with the DNA-binding domain of FEZF2 (*pCAG-Fezf2-VP16*) (Supplemental Figure 2a). We co-electroporated each plasmid with a *pCAG-EGFP* plasmid into the cortical ventricular zone of E15.5 wild-type embryos and examined the brains at P5 (Supplemental Figure 2b). In all the electroporated brains, GFP^+ neurons were located in layers 2/3 and GFP^+ callosal axons were observed. GFP^+ axons were not detectable in the thalamus or pons of brains electroporated with the *pCAG-EGFP* plasmid alone, nor in brains electroporated with *pFezf2-VP16* plasmids. However, both full-length FEZF2 and FEZF2-EnR directed layer 2/3 neurons to project GFP^+ axons into the thalamus and cerebral peduncle (Supplemental Figure 2b).

To ascertain whether FEZF2 functions primarily as a transcriptional repressor during deep layer neuronal differentiation, we generated a transgenic line expressing the FEZF2-EnR chimeric protein using a bacterial artificial chromosome (BAC) (Figure 2a). This BAC consisted of a 200kb region flanking the *Fezf2* gene. We inserted the FEZF2-EnR open reading frame at the endogenous *Fezf2* translation start site, immediately followed by a transcription termination signal. Western blot analysis confirmed that endogenous FEZF2 protein was not expressed from the *Fezf2-EnR* transgenic allele (Figure 2b). Immunostaining showed that expression of the FEZF2-EnR protein recapitulates that of endogenous *Fezf2* (Figure 2c).

We then determined whether FEZF2-EnR can rescue the defects resulting from a loss of *Fezf2* by comparing the brains of *Fezf2*$^{+/-}$, *Fezf2*$^{-/-}$, and *Fezf2*$^{-/-}$*; Fezf2-EnR* mice (Figure 2d-i, Supplemental Figures 2c-e and 3). The expression patterns of subcerebral neuronal markers such as BCL11B, BHLHB5 (Figure 2d-e, g), *Tox*, *Tcerg1*, and *Ldb2* (Supplemental Figure 3) were restored in layer 5 neurons in *Fezf2*$^{-/-}$*; Fezf2-EnR* mice. Similarly, the expression patterns of corticothalamic neuronal genes such as TLE4, FOXP2 (Supplemental Figure 2c-e) and ZFPM2 (data not shown), and of the subplate neuronal gene *Ctgf* (Supplemental Figure 3) were restored. The ectopic expression of TBR1 (data not shown), FOSL2 (Supplemental Figure 2c), and SATB2 (Figure 2d,f) in layer 5 was no longer detected. Further, PLAP^{+} axons projected into the pyramidal decussation, the dLGN and other thalamic nuclei

in the *Fezf2*$^{-/-}$*; Fezf2-EnR* mice (Figure 2i). Thus, the *Fezf2-EnR* allele fully rescued the defects observed in layer 5, layer 6, and subplate neurons in *Fezf2*$^{-/-}$ mice, demonstrating that FEZF2 functions as a transcriptional repressor.

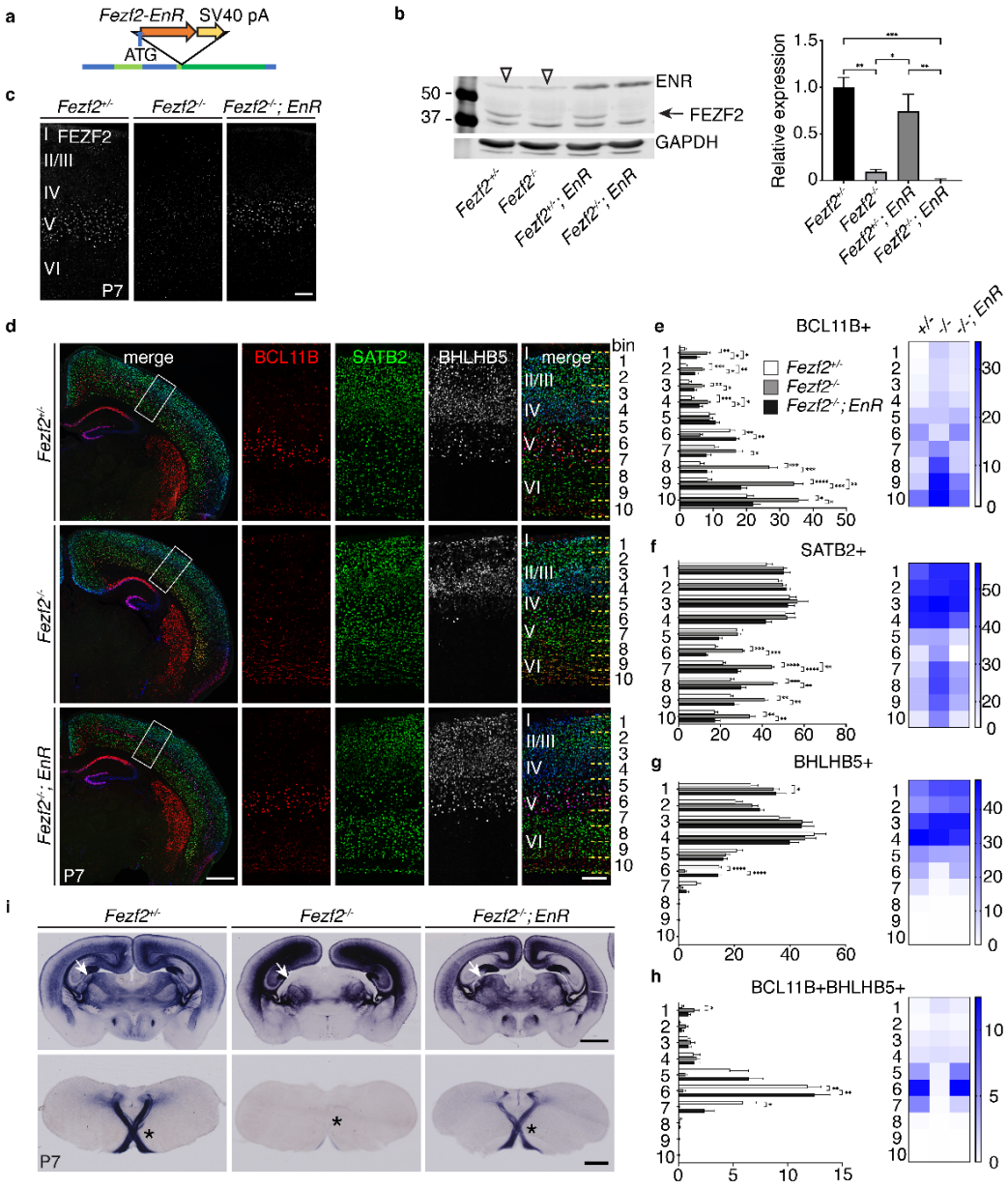

Figure 2: FEZF2 functions as a transcriptional repressor in cortical development.

a. Strategy for generating the *Fezf2-EnR* BAC transgenic mouse line. **b**. Western blot analysis of dissected cortices at P7. FEZF2 signal was normalized to GAPDH signal in each lane. n = 3 brains per genotype. arrow: FEZF2 protein; empty triangles: non-specific bands. **c**. Immunostaining for FEZF2 on brain sections from P7 *Fezf2*$^{+/-}$, *Fezf2*$^{-/-}$, and *Fezf2*$^{-/-}$; *Fezf2-EnR* (*EnR*) mice. scale bar: 100 μm. **d**. Immunostaining for BCL11B, SATB2, and BHLHB5 on P7 brain sections. scale bar for low magnification: 500 μm. scale bar for high magnification: 100 μm. **e-h**. Quantifications of marker^{+} cells per 10,000 μm^{2} in each bin. Heatmaps show the

mean numbers of cells per 10,000 um^2 for each bin. n=3 mice per genotype, 3 sections per brain. In all graphs, error bars represent ± SEM. Statistical significance was determined using one-way ANOVA followed by post hoc Tukey's t-test (*p<0.05, **p<0.01, ***p<0.001, ****p<0.0001). Binning was shown in d. **i**. PLAP staining of brain sections of P7 *Fezf2*$^{+/-}$, *Fezf2*$^{-/-}$, *Fezf2*$^{-/-}$*; EnR mice*. The top row shows coronal cortical sections, the bottom row shows coronal sections at the level of pyramidal decussation. Scale bars: 1 mm for top row, 500 μm for bottom row. arrows: LGN; *: pyramidal decussation.

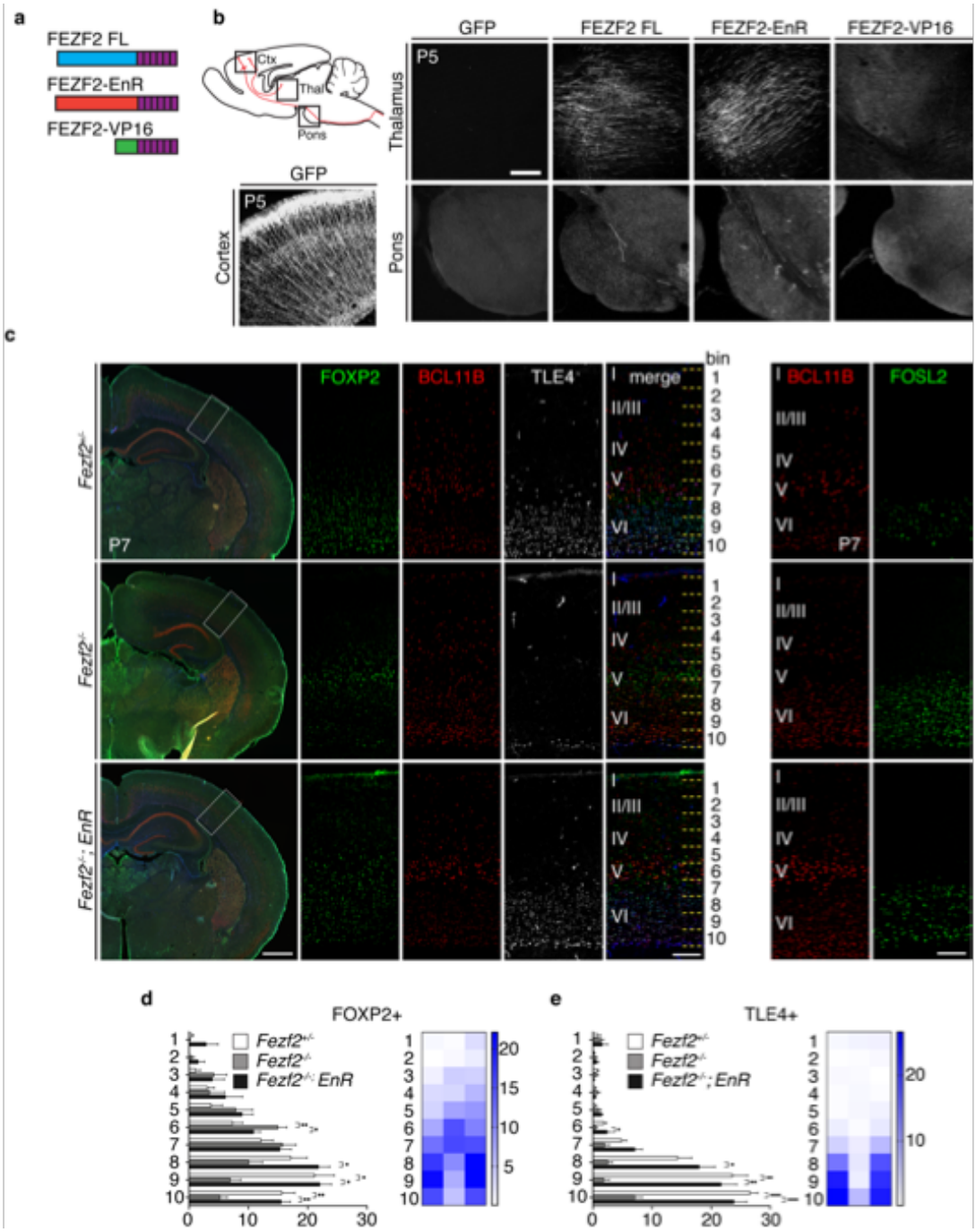

Figure S2. FEZF2 functions as a transcriptional repressor during cortical development.

a. Schematic representations of full-length FEZF2 protein, the FEZF2-EnR chimeric protein, and the FEZF2-VP16 chimeric protein. blue: the N-terminal half of FEZF2; purple: the 6 C2H2-type zinc finger motifs of FEZF2; red: the EnR transcriptional repressor domain; green: the VP16 transcriptional activator domain. **b**. Over-

expression of full-length FEZF2, FEZF2-EnR, and FEZF2-VP16 into layer 2/3 neurons by *in utero* electroporation at E15.5, and the effect on axonal projection was assessed at P5 using GFP immunostaining. GFP labeled cells and axons in three boxed areas (cortex, thalamus and pontine nuclei) were shown. Scale bar, 200 μm. **c**. Immunostaining of FOXP2, BCL11B, TLE4 and FOSL2 in brains of P7 *Fezf2*$^{+/-}$, *Fezf2*$^{-/-}$, and *Fezf2*$^{-/-}$*; EnR* mice. Scale bars: low mag, 500 μm, high mag 100 μm. **d-e**. Quantifications of marker^{+} cells per 10,000 μm^2 per bin. n=3 brains per genotype, 3 sections per brain. In all graphs, error bars represent ± SEM. Statistical significance was determined using one-way ANOVA followed by post hoc Tukey's t-test (*p<0.05, **p<0.01, ***p<0.001). Heatmaps show mean numbers of cells per 10,000 um^2 for each bin.

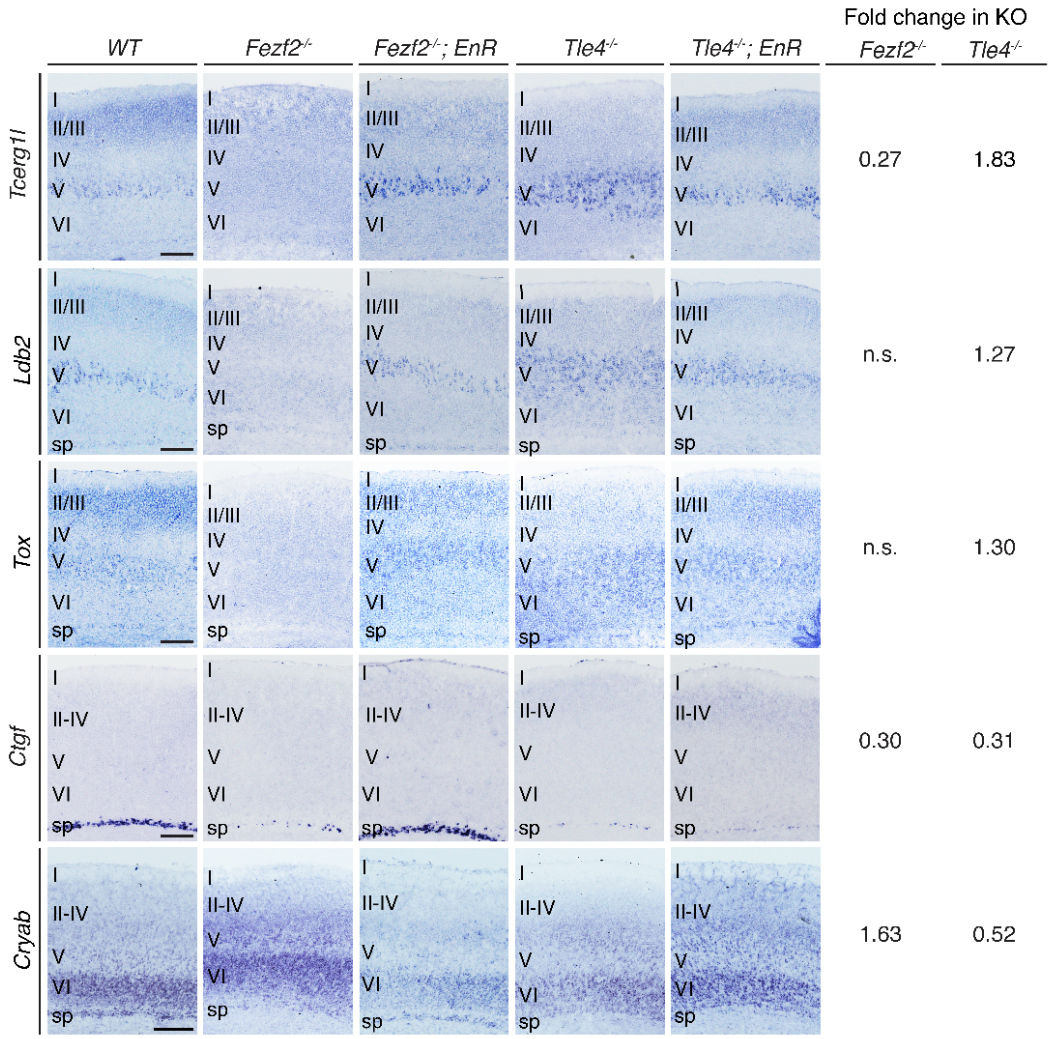

Figure S3. *In situ* hybridization showed that *Fezf2*-EnR fully rescued the molecular defects in cortical projection neurons of the *Fezf2*$^{-/-}$ mice, and prevented increased expression of subcerebral neuronal genes in the *Tle4*$^{-/-}$ mice.

In situ hybridizations for *Ctgf, Cryab, Tcerg1l, Ldb2,* and *Tox* on 20 μm thick P7 coronal sections from *wt, Fezf2*$^{-/-}$, *Fezf2*$^{-/-}$*; EnR, Tle4*$^{-/-}$, *Tle4*$^{-/-}$*; EnR* mice. The fold change in expression level in *Fezf2*$^{-/-}$ cortices compared to wild-type littermate controls, and in *Tle4*$^{-/-}$ cortices compared to wild-type littermate controls is shown in the two right columns. sp: Subplate. Scale bars: 200 μm.

Subtype-specific genes are mis-regulated in the *Fezf2*$^{-/-}$ cortices

To further investigate how FEZF2 regulates projection subtype identities, we performed bulk RNA-seq analysis of cortices from P0 *Fezf2*$^{-/-}$ and littermate control *Fezf2*$^{+/+}$ mice (n=3 mice for each genotype). The expression levels of 390 genes were mis-regulated in the *Fezf2*$^{-/-}$ cortices ($P<0.05$). 221 genes showed reduced expression and 169 showed increased expression. DAVID analysis (https://david.ncifcrf.gov) revealed that the top GO terms associated with mis-regulated genes in *Fezf2*$^{-/-}$ cortices were extracellular region, multicellular organism development, collagen fibril organization, synapse, and cell junction. We examined the expression of these mis-regulated genes in specific subtypes of cortical neurons using the DeCoN dataset (www.decon.fas.harvard.edu; Molyneaux et al., 2015), and found that 161 of the 221 genes showing reduced expression in *Fezf2*$^{-/-}$ cortices were subtype-specific ($\chi^2=256.1$, DF=3, $P<<0.001$): 77 genes were enriched in subcerebral neurons, 77 in corticothalamic neurons, and 7 in corticocortical neurons. Among the 169 genes showing increased expression in *Fezf2*$^{-/-}$ cortices, 135 were subtype-specific ($\chi^2=308.2$, DF=3, $P<<0.001$): 90 were enriched in corticocortical neurons, 28 in corticothalamic neurons, and 17 in subcerebral neurons (Figure 3a). We confirmed the subtype-specific expression of some of these genes using the Allen Brain Atlas (http://developingmouse.brain-map.org/) and performing *in situ* hybridization

(Figure 3b-d). These results suggest that FEZF2 primarily regulates subtype-specific gene expression.

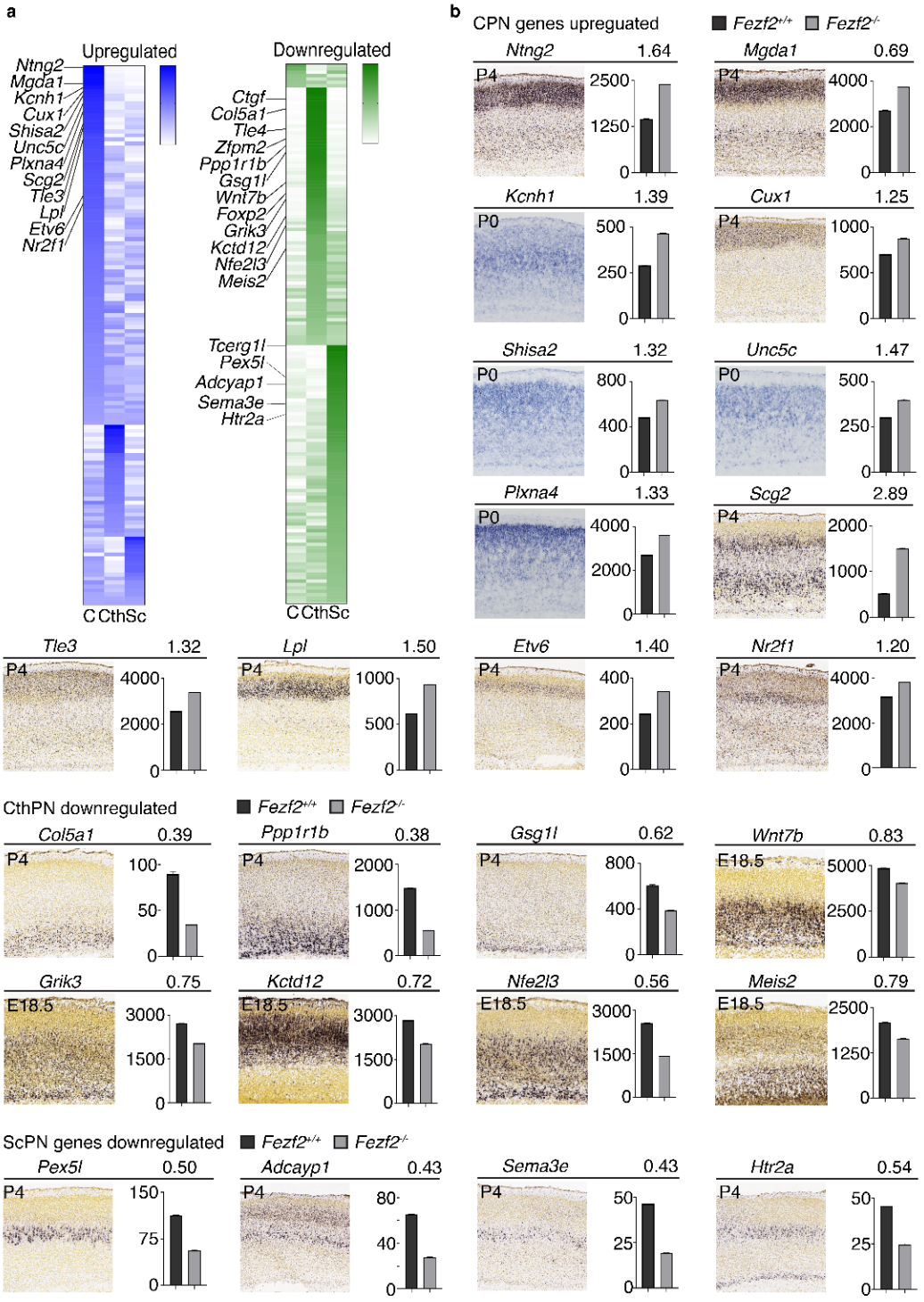

Figure 3: Genes mis-regulated in *Fezf2*$^{-/-}$ cortices were enriched in projection neuron subtype-specific genes.

a. Left heatmap shows genes with increased expression in *Fezf2*$^{-/-}$ cortices. Right heatmap shows genes with decreased expression in *Fezf2*$^{-/-}$ cortices. Heatmaps for

the mis-regulated genes were generated based on relative expression levels in each respective cell type at P1 from the DeCoN dataset. C: callosal neuronal genes; Cth: corticothalamic neuronal genes; Sc: subcerebral neuronal genes. **b-d**. Expression patterns detected by *in situ* hybridizations and fold of change of expression level in the *Fezf2*$^{-/-}$ cortices for the up-regulated callosal neuronal genes, and down-regulated corticothalamic and subcerebral neuronal genes. All the *in situs* except *Kcnh1*, *Shisa2*, *Unc5c* and *Plxn4* were from the Allen Brain Atlas Developing Mouse Brain data.

TLE4 and FEZF2 are co-expressed in differentiating corticothalamic neurons

The N-terminal of the FEZF2 protein contains an EH1 motif, which recruits the TLE family co-repressors (Muhr et al., 2001). A previous study reported that Xenopus FEZF2 and TLE4 proteins directly interact with each other (Zhang et al., 2014). To determine whether FEZF2 recruits TLE4 to regulate the development of deep-layer neurons, we first performed immunostaining using antibodies against FEZF2 and TLE4, which revealed that the two proteins were co-expressed in layer 6 neurons (Figure 4a).

To identify the neuronal subtype that expresses TLE4, we performed retrograde tracing by injecting fluorescence-conjugated cholera toxin beta subunit (CTB) into the thalamus, pyramidal decussation, or contralateral cortex (Figure 4b). More than 99% of retrogradely labeled corticothalamic neurons expressed TLE4, whereas labeled subcerebral neurons and callosal neurons did not (<1%). Thus, TLE4 is specifically expressed in corticothalamic neurons.

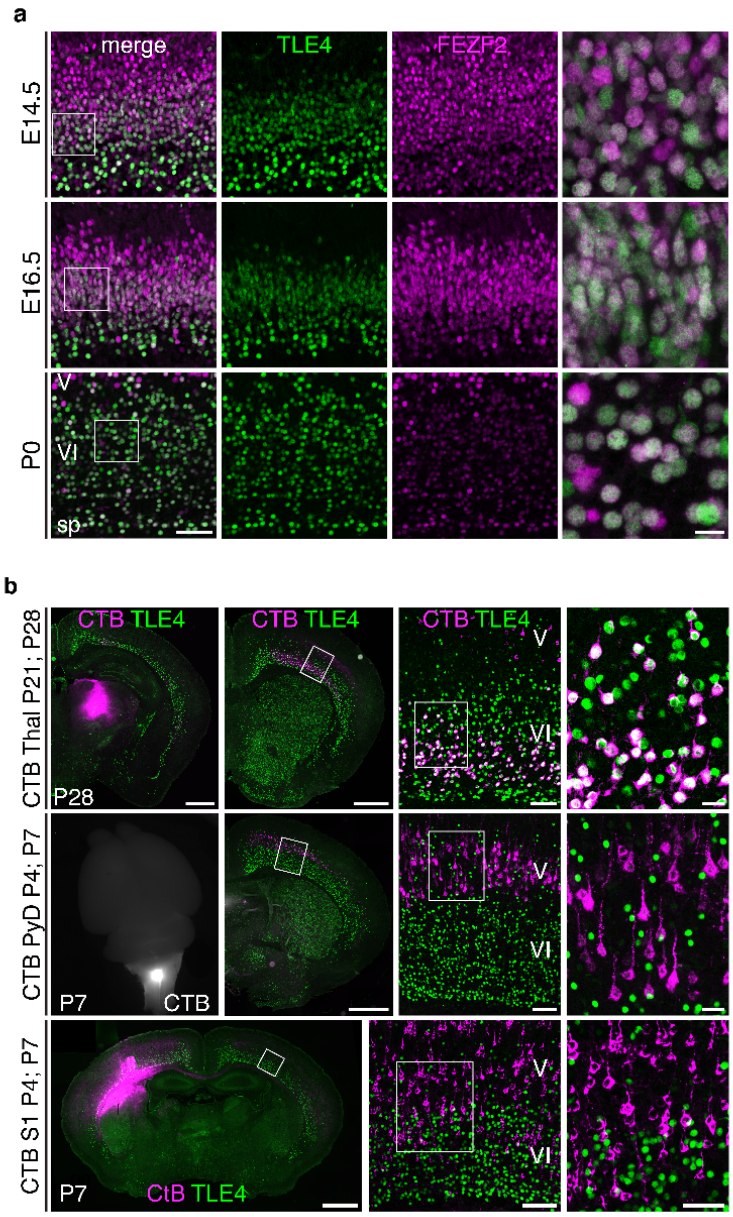

Figure 4: TLE4 and FEZF2 are co-expressed in corticothalamic neurons. **a**. Immunostaining for TLE4 and FEZF2 at E14.5, E16.5 and P0 in WT mice. Low mag: single z-plane image, scale bar 50 μm, high mag: maximum z-projection image, scale bar 10μm. **b.** Retrograde tracing and immunostaining show TLE4 is expressed in >99% of retrogradely labeled CThPNs in M1 (1034 $TLE4^{+}CTB^{+}$ /1050 CTB^{+} cells), 0% of the traced SCPNs (930 cells), and 0.1% of the CPNs (2 $TLE4^{+}CTB^{+}$ among 1783 CTB^{+} cells). n=3 mice for each injection location, and 3 sections per brain were quantified.

Corticothalamic axons developed normally in the *Tle4*$^{-/-}$ mice

To test the function of *Tle4* in the specification and differentiation of corticothalamic neurons, we generated a *Tle4* mutant allele by inserting a *BGal-ires-Plap* cassette into the 4th intron of the *Tle4* gene (Supplemental Figure 4a). The BGAL and PLAP reporters enabled us to label the cell bodies and axons of *Tle4* heterozygous and mutant neurons, respectively (Supplemental Figure 4b, d). In *Tle4*$^{+/-}$ brains, BGAL expression recapitulated the endogenous pattern of TLE4 expression (Supplemental Figure 4b). Immunostaining revealed that TLE4 protein is not present in *Tle4*$^{-/-}$ mice (Supplemental Figure 4c). In both *Tle4*$^{+/-}$ and *Tle4*$^{-/-}$ mice, PLAP^{+} axons extended from cortex to the thalamus, with no obvious difference between control and mutant brains (Supplemental Figure 4d). We performed anterograde tracing by injecting AAV-mcherry virus into the M1, S1, and V1 cortical areas, which confirmed that corticothalamic axons developed normally in *Tle4*$^{-/-}$ mice (Supplemental Figure 4e and data not shown).

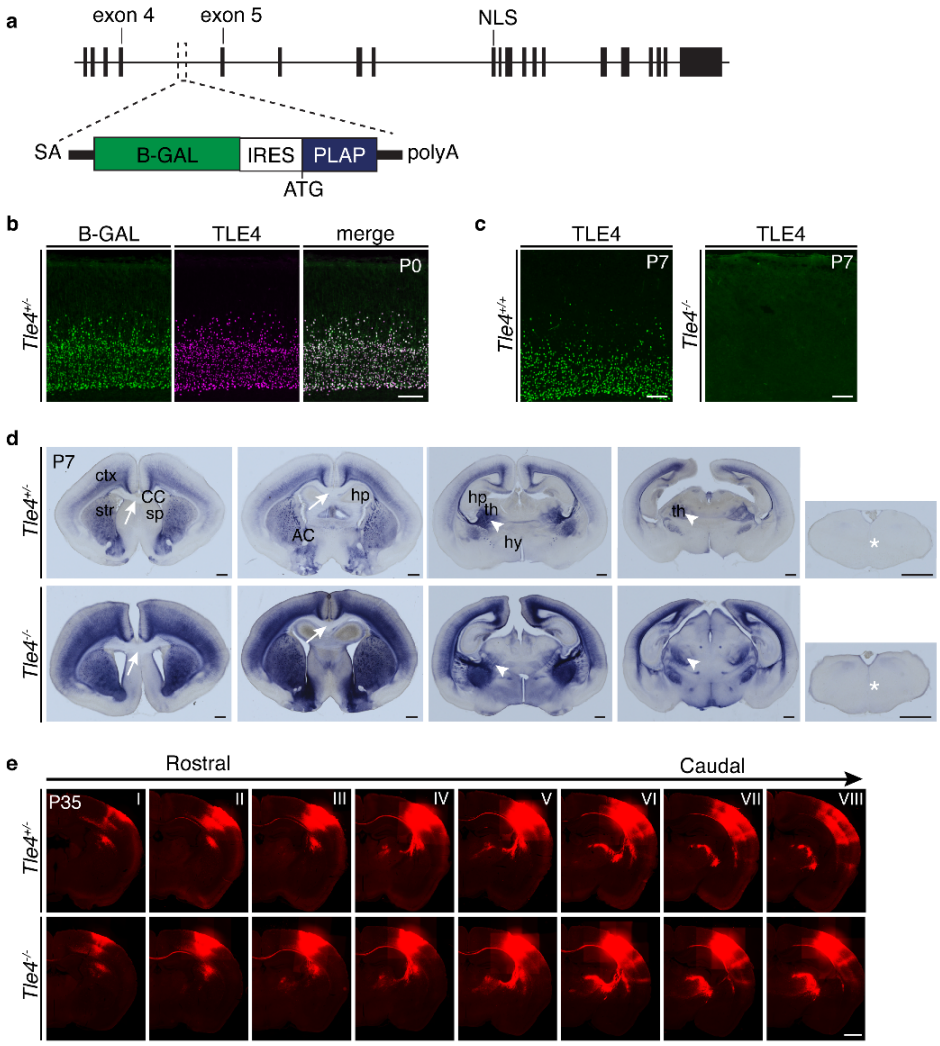

Figure S4. Corticothalamic neurons project axons properly into the thalamus of *Tle4*$^{-/-}$ mice.

a. Knockout strategy for *Tle4* gene. SA-B-Gal-ires-Plap cassette was inserted into the intron after exon 4. *SA*: splicing acceptor; *B-Gal*: β-galactosidase; *ires*:internal ribosome entry site; *Plap*: human placental alkaline phosphatase; *NLS:* nuclear localization signal. **b**. Staining shows that B-GAL recapitulates TLE4 expression in the *Tle4*$^{+/-}$ mice. scale bar:100 µm **c**. TLE4 protein is not detected by immunostaining in the *Tle4*$^{-/-}$ mice. **d**. PLAP staining of P7 *Tle4*$^{+/-}$ and *Tle4*$^{-/-}$ mice. arrows: corpus callosum; arrowheads: thalamus; *: pyramidal decussation. Scale bars: 500µm. AC: anterior commissure; ctx: cerebral cortex, CC: corpus callosum, str: striatum, sp: septum, hp: hippocampus; hy: hypothalamus; th: thalamus. **e**. AAV-mCherry was injected into primary somatosensory cortex in *Tle4*$^{+/-}$ and *Tle4*$^{-/-}$ mice at P21, brains collected at P35. Eight consecutive 50µm sections (I-VIII) shown. Scale bar:1mm.

Molecular differentiation of corticothalamic neurons is defective in *Tle4*$^{-/-}$ mice

We performed RNA-seq analysis of control and *Tle4*$^{-/-}$ P0 cortices (n=3 mice for each genotype). 473 genes were mis-regulated in the *Tle4*$^{-/-}$ cortices ($P<0.05$, student's t-test). Using the DeCoN dataset (http://decon.fas.harvard.edu/), we examined the neuronal subtype-specific expression of all mis-regulated genes. Among the 253 genes with reduced expression, 27 were associated with corticocortical neurons, 79 were specifically expressed in corticothalamic neurons and 18 in subcerebral neurons. Among the 220 up-regulated genes, 29 were associated with corticocortical neurons, 69 were enriched in subcerebral neurons and 24 in corticothalamic neurons (Figure 5a).

We performed immunohistochemistry and *in situ* hybridization to validate the RNA-seq results. Consistent with the normal corticothalamic axons observed in *Tle4*$^{-/-}$ brains, the expression of TBR1 and SOX5, two genes essential for specifying a corticothalamic neuron identity, was not significantly affected in mutant mice (Supplemental Figure 5a-b). However, the number of BGAL^{+} neurons was significantly reduced in layer 5 and layer 6a in *Tle4*$^{-/-}$ mice (Figure 5b). Expression of other layer 6 neuron markers such as ZFPM2 (Figure 5b) and FOXP2 (Supplemental Figure 5c) was also significantly reduced. High expression levels of FEZF2, BCL11B, BHLHB5, *Ldb2, Tcerg1l,* and *Tox* are normally associated with layer 5 subcerebral

neurons, but in *Tle4*$^{-/-}$ mice, their expression was significantly increased in layer 6 (Figure 5c-d and Supplemental Figure 3).

The reduced numbers of BGAL^{+}, ZFPM2^{+}, and FOXP2^{+} cells in *Tle4*$^{-/-}$ mice could be due to reduced neuronal production, increased cell death, or defective molecular differentiation, while the increased numbers of cells expressing BCL11B, FEZF2, and other subcerebral markers in layer 6 could be due to a migration defect of layer 5 neurons or the mis-regulation of these genes in layer 6 neurons. To ascertain whether the production or migration of layer 5 and 6 neurons was affected in *Tle4*$^{-/-}$ mice, we performed birthdating experiments by injecting EdU into pregnant mice on E12.5 or E13.5, and analyzing the brains of *Tle4*$^{-/-}$ and control mice at P7. For both labeling dates, we saw no significant change in the number or distribution of EdU^{+} cells in the deep layers of *Tle4*$^{-/-}$ cortices (Supplemental Figure 6a-b). We then stained control and *Tle4*$^{-/-}$ sections at E14, P0 and P7 with an antibody against activated caspase 3 (AC3) and saw no significant difference in the number of AC3^{+} cells between genotypes at any age (Supplemental Figure 6c).

Together, these results indicate that in *Tle4*$^{-/-}$ mice, corticothalamic neurons were generated in appropriate numbers, migrated to their normal laminar destinations, and projected axons to the thalamus. However, the molecular differentiation of these neurons was impaired, resulting in the expression of genes normally associated with subcerebral neurons.

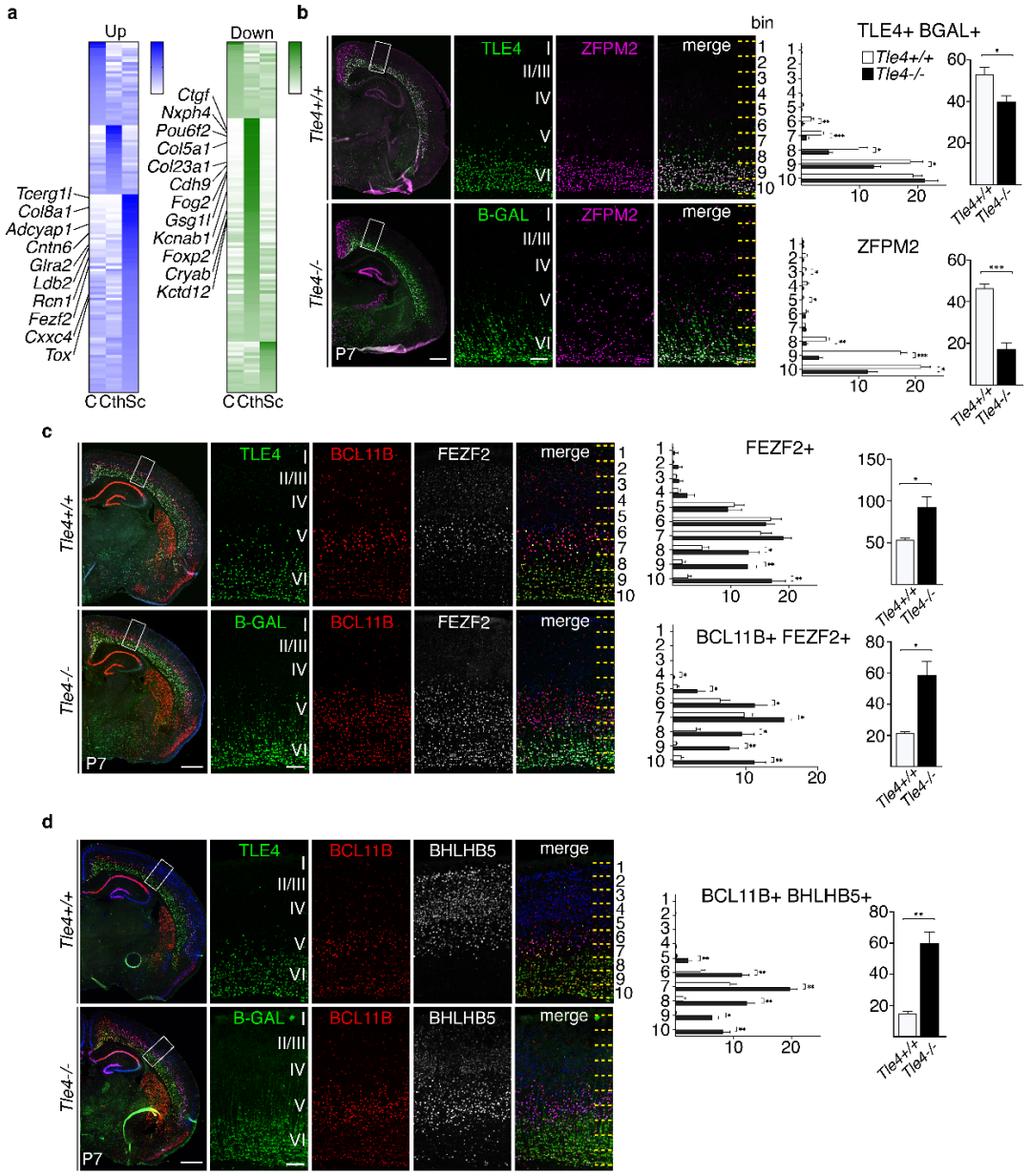

Figure 5. Molecular differentiation of corticothalamic neurons was defective in *Tle4*$^{-/-}$ brains.

a. RNA-seq revealed that genes with increased expression in *Tle4*$^{-/-}$ cortices are enriched in subcerebral neuronal genes, while those reduced expression were enriched in corticothalamic neuronal genes. Left heatmap shows genes increased in *Tle4*$^{-/-}$ cortices. Right heatmap shows genes decreased in *Tle4*$^{-/-}$ cortices. Heatmaps for the mis-regulated genes were generated based on relative expression levels in each respective cell type at P1 from the Decon dataset. C: callosal neuronal genes; Cth: corticothalamic neuronal genes; Sc: subcerebral neuronal genes. **b**.

Immunostaining of TLE4 or B-GAL and ZFPM2 in the P7 brains, and quantifications of the numbers of $TLE4^+$ or $B\text{-}GAL^+$, and $ZFPM2^+$ cells by bin, and total cell counts. **c**. Immunostaining of TLE4 or B-GAL, BCL11B, and FEZF2 in the P7 brains, and quantifications of the $FEZF2^+$ and $BCL11B^+FEZF2^+$ cells by bin, and total cell counts. **d**. Immunostaining of TLE4 or B-GAL, BCL11B, and BHLHB5 in the P7 brains, and quantifications of the $BCL11B^+BHLHB5^+$ cells n=3 brains per genotype, 3 sections per brain. Quantifications of $marker^+$ cells per 10,000 μm^2 in each bin. In all graphs, error bars represent ± SEM. Statistical significance was determined using unpaired student's t-tests (*p<0.05, **p<0.01, ***p<0.001). Scale bars: low mag, 1 mm, low mag, 500 μm.

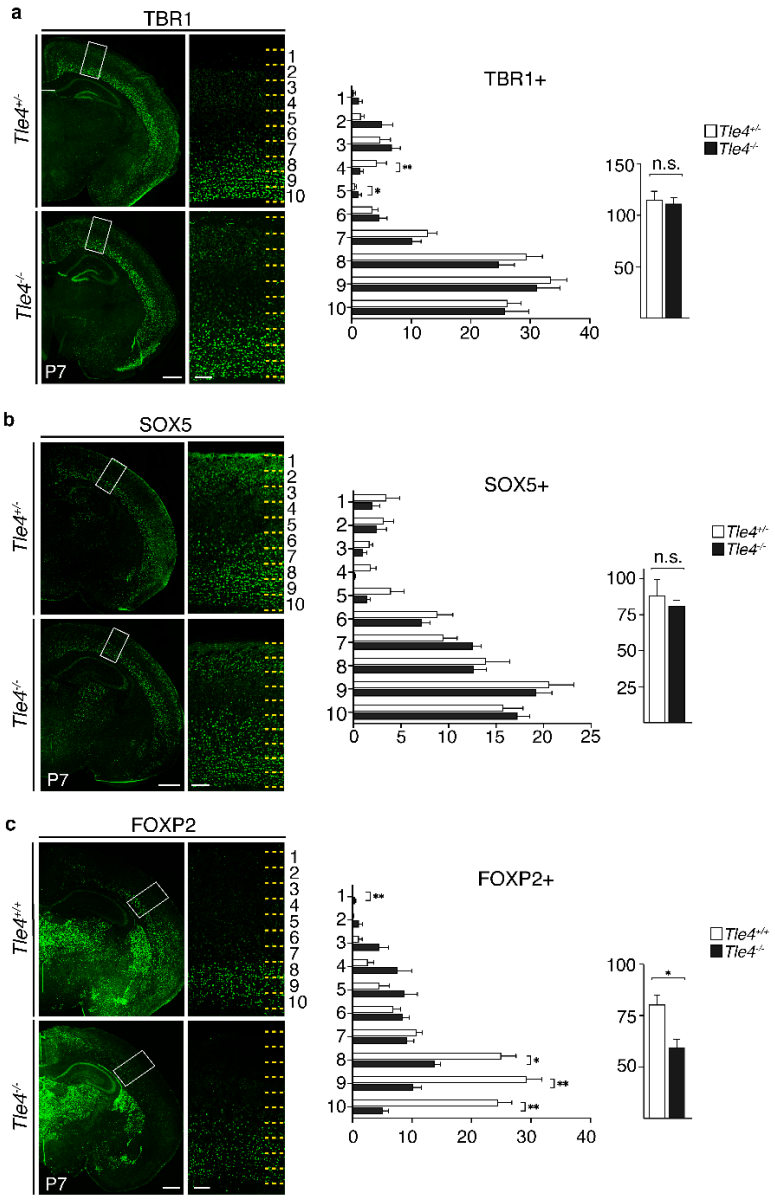

Figure S5. The numbers of TBR1$^+$ and SOX5$^+$ layer 6 neurons were not affected in *Tle4*$^{-/-}$ cortices, while the number of FOXP2$^+$ cells was reduced.
a. TBR1 staining, quantification by bin and the total numbers of TBR1$^+$ cells in *Tle4*$^{+/-}$ and *Tle4*$^{-/-}$ cortices. **b**. SOX5 staining, quantification by bin and the total numbers of SOX5$^+$ cells in *Tle4*$^{+/-}$ and *Tle4*$^{-/-}$ cortices. **c**. FOXP2 staining, quantification by bin and the total numbers of FOXP2$^+$ cells in *Tle4*$^{+/+}$ and *Tle4*$^{-/-}$ cortices. n=3 brains per genotype, 3 sections per brain. Quantifications of marker$^+$ cells per 10,000 μm^2 in each bin. In all graphs, error bars represent ± SEM. Scale bars: low mag, 500 μm, high mag 100 μm.

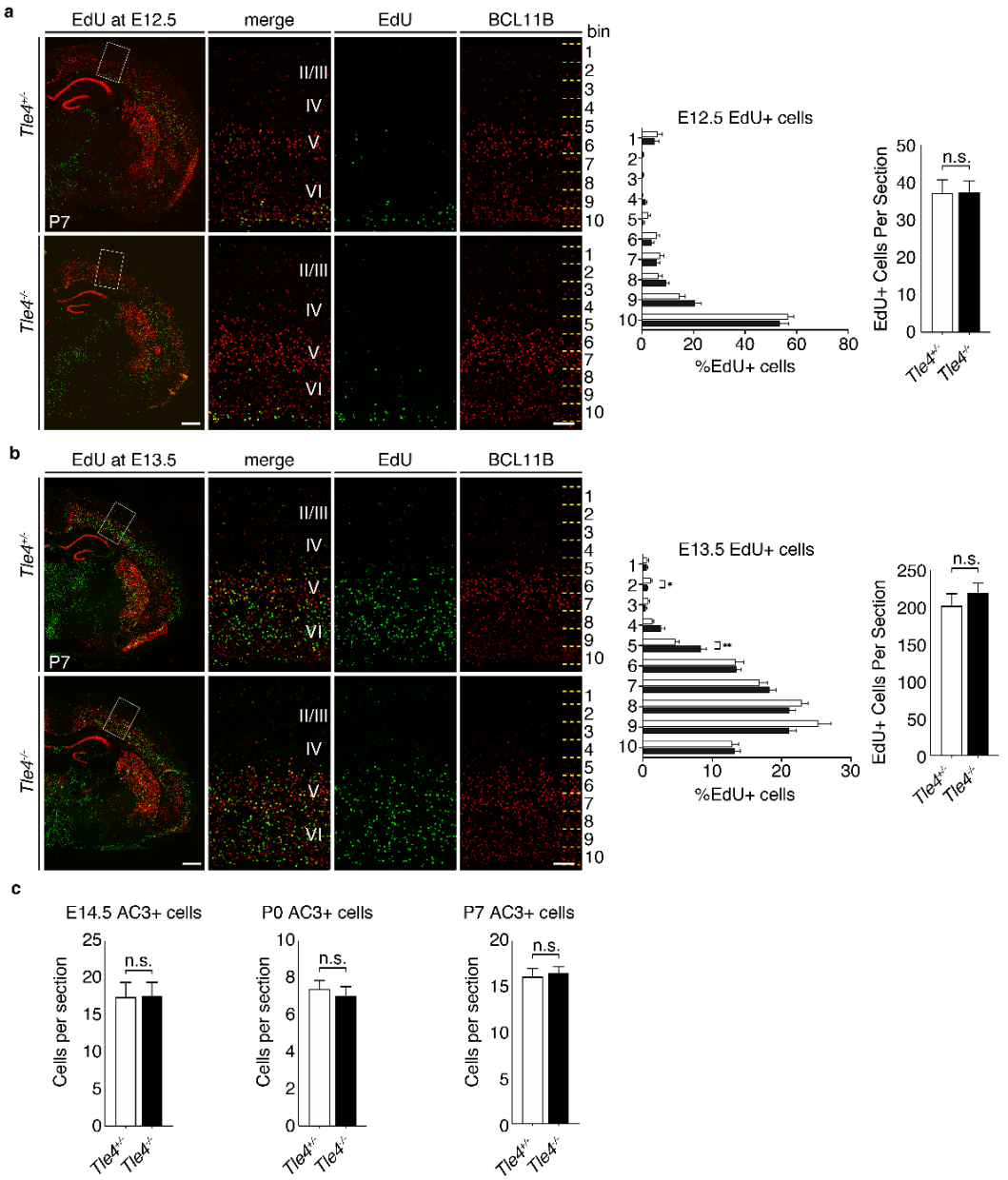

Figure S6. EdU birthdating and apoptosis analysis of the *Tle4*$^{+/+}$ and *Tle4*$^{-/-}$ cortices.

a. EdU was given at E12.5, brains were analyzed at P7. Quantifications show the %EdU^{+} cells per bin, and EdU^{+} cells per 750 µm wide section. **b**. EdU was given at E13.5, brains were analyzed at P7. Quantifications show the %EdU^{+} cells per bin, and total numbers of EdU^{+} cells per 500 µm wide section. **c**. Quantifications of AC3^{+} cells per section at E14.5, P0 and P7. n=3 mice per genotype, 3 sections per brain. Statistical significance for quantifications in **a-c** were determined using the unpaired student's t-test (*p<0.05, **p<0.01).

Morphological and electrophysiological defects of corticothalamic neurons in *Tle4*$^{-/-}$ mice

We next investigated whether *Tle4* is required for the morphological and functional differentiation of corticothalamic neurons. We injected retrobeads into the ventral posteromedial nucleus (VPM) of the thalamus (Landisman et al., 2007) of *Tle4*$^{+/+}$ and *Tle4*$^{-/-}$ mice (P27-35), and performed whole cell patch clamp recordings and morphological analyses on labeled corticothalamic neurons in primary somatosensory cortex (S1) (Figure 6a-b). Sholl analysis on reconstructed dendritic arbors revealed a significant reduction in the branching ($F_{(2,286)} = 3.4$, $p = 0.034$) and length ($F_{(2,253)} = 7.3$, $p = 0.0009$) of dendrites in mutant mice (Figure 6c). Mutant corticothalamic neurons also show significantly increased spine density, decreased spine head diameter, and increased spine length (Figure 6d).

Patch clamp recordings revealed that corticothalamic neurons in *Tle4*$^{-/-}$ mice exhibited increased excitability, as demonstrated by an increased number of action potentials (AP) firing in response to current steps (Figure 6e, $F_{(1,110)} = 38.9$, $p < 0.001$); however, the AP threshold was unaffected (Figure 6f). Mutant corticothalamic neurons showed an increased membrane resistance and decreased membrane capacitance (Figure 6g, $p < 0.05$ for both). The amplitude ($p = 0.02$, K-S test) and frequency ($t_{31} = 2.7$, $p = 0.011$) of miniature excitatory postsynaptic currents (mEPSC) were reduced in *Tle4*$^{-/-}$

mice compared to wild-type mice (Figure 6h), but no significant change in the amplitude or frequency of miniature inhibitory postsynaptic currents (mIPSC) was observed (Figure 6i). These results collectively indicate that *Tle4* is critical for the morphological development and function of corticothalamic neurons in somatosensory cortex.

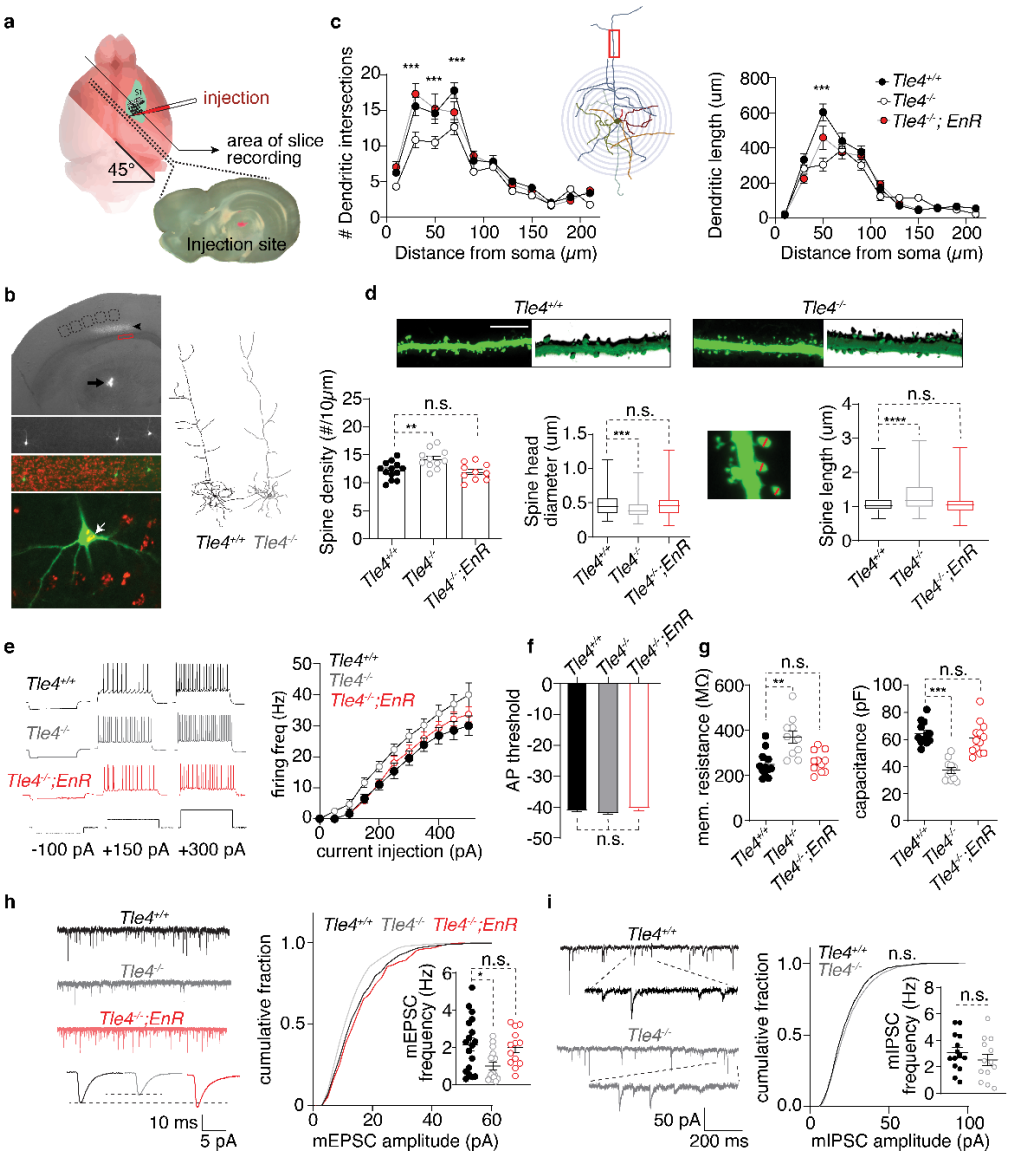

Figure 6. *Tle4*$^{-/-}$ mice show disrupted morphological and electrophysiological properties in corticothalamic neurons in S1, which were rescued by the *Fezf2-EnR* allele.

a. Schematic illustration of retrobeads injection into VPM of thalamus, and preparation of S1 slices for patch clamp recording. **b**. A brightfield image overlaid with bead^{+} layer 6 corticothalamic neurons. An enlarged view shows a beads^{+} corticothalamic neuron and its morphology revealed by biocytin-avidin-Alexa 488. *Right,* two examples of representative dendritic arbors reconstructed from the beads^{+} corticothalamic neurons in a *Tle4*$^{+/+}$ and a *Tle4*$^{-/-}$ mouse. **c**. Sholl analysis on the dendritic intersection numbers and dendritic length. *Left* panel shows a significant

difference among the genotypes ($F_{(2, 297)}$ = 21.7, p < 0.0001. Tukey's multiple comparison tests: between *Tle4*$^{+/+}$ and *Tle4*$^{-/-}$ mice, p < 0.0001; between *Tle4*$^{+/+}$ and *Tle4*$^{-/-}$; *Fezf2-EnR* mice, p = 0.96. ***p < 0.001, between *Tle4*$^{+/+}$ and *Tle4*$^{-/-}$ mice, Sidak's multiple comparison test). *Right* panel shows dendritic length distribution. Genotype has a significant effect ($F_{(2, 253)}$ = 7.54, p = 0.0007. Tukey's multiple comparisons test: between *Tle4*$^{+/+}$ and *Tle4*$^{-/-}$, p = 0.0006; between *Tle4*$^{+/+}$ and *Tle4*$^{-/-}$; *Fezf2-EnR*, p = 0.42. ****p < 0.0001, between *Tle4*$^{+/+}$ and *Tle4*$^{-/-}$, Sidak's multiple comparison test). **d**. Representative images of dendritic spines and their 3-D projection images. Compared to the *Tle4*$^{+/+}$ neurons, there was a significant increase in spine density (**p = 0.007, one way ANOVA with Dunnett's multiple comparison) and spine length (**** p < 0.0001, Kruskal-Wallis test followed by Dunn's multiple comparison test), and a significant decrease in spine head diameter (** p < 0.0013) for the *Tle4*$^{-/-}$ corticothalamic neurons. No significant difference in spine density, spine length, or spine head diameter was detected between the corticothalamic neurons in *Tle4*$^{+/+}$ and *Tle4*$^{-/-}$; *Fezf2-EnR* mice. **e**. Representative action potential firing responses from a *Tle4*$^{+/+}$, *Tle4*$^{-/-}$, and a *Tle4*$^{-/-}$; *Fezf2-EnR* corticothalamic neuron. Genotype has a significant effect on the current-AP responses ($F_{(2, 165)}$ = 24.1, p < 0.0001). Compared to *Tle4*$^{+/+}$ neurons, *Tle4*$^{-/-}$ neurons show increased firing in response to depolarizing current steps (p < 0.0001, Dunnett's multiple comparison), which was reversed in *Tle4*$^{-/-}$; *Fezf2-EnR* mice (p = 0.14). **f**. AP threshold did not differ between *Tle4*$^{+/+}$, *Tle4*$^{-/-}$, or *Tle4*$^{-/-}$; *Fezf2-EnR* neurons ($F_{(2,32)}$ = 2.5, p = 0.09, one-way ANOVA with Dunnett's multiple comparison). **g**. Genotype has a significant effect on membrane input resistance ($F_{(2,30)}$ = 10.8, p = 0.0003, one-way ANOVA). *Tle4*$^{-/-}$ neurons show increased input resistance compared to *Tle4*$^{+/+}$ neurons (p = 0.0003, Dunnett's multiple comparison test), which was rescued in *Tle4*$^{-/-}$; *Fezf2-EnR* mice (p = 0.87). Genotype has a significant effect on membrane capacitance ($F_{(2,33)}$ = 28.0, p < 0.0001). Compared to *Tle4*$^{+/+}$ neurons, *Tle4*$^{-/-}$ neurons show decreased membrane capacitance (p = 0.0003, Dunnett's multiple comparison test), which was rescued in *Tle4*$^{-/-}$; *Fezf2-EnR* mice (between *Tle4*$^{+/+}$ and *Tle4*$^{-/-}$; *Fezf2-EnR:* p = 0.52). **h**. *Left,* Representative mEPSC traces from *Tle4*$^{+/+}$, *Tle4*$^{-/-}$, and *Tle4*$^{-/-}$; *Fezf2-EnR* neurons. *Right,* cumulative plot on mEPSC amplitude. Between *Tle4*$^{+/+}$ and *Tle4*$^{-/-}$, *p < 0.02, Kolmogov-Smirnov test; between *Tle4*$^{-/-}$ and *Tle4*$^{-/-}$; *Fezf2*-EnR, p = 0.57. Inset, a significant decrease in mEPSC frequency in *Tle4*$^{-/-}$ neurons (between *Tle4*$^{+/+}$ and *Tle4*$^{-/-}$, * p = 0.015, Dunn's multiple comparison following Kruskal-Wallis test) was restored by the *Fezf2*-EnR allele (between *Tle4*$^{+/+}$ and *Tle4*$^{-/-}$*; Fezf2-EnR*: p = 0.99, Dunn's multiple comparison test). **i**. No significant change in mIPSC amplitude and frequency was observed between *Tle4*$^{+/+}$ and *Tle4*$^{-/-}$ neurons (cumulative amplitude: p = 0.43; frequency: p = 0.17. Kolmogov-Smirnov test.)

Expression of FEZF2-EnR rescued the molecular, morphological, and functional defects of layer 6 neurons in *Tle4*$^{-/-}$ cortices

The co-expression of FEZF2 and TLE4 in corticothalamic neurons suggests that they function together in regulating the development of these neurons. To test this, we generated *Tle4*$^{-/-}$*; Fezf2-EnR* mice and compared them to *Tle4*$^{+/+}$ and *Tle4*$^{-/-}$ mice. The number of B-GAL^{+} cells in *Tle4*$^{-/-}$*; Fezf2-EnR* mice was restored to the number of TLE4^{+} cells seen in *Tle4*$^{+/+}$ mice (Figure 7a-b). The expression of genes normally enriched in subcerebral neurons, such as BCL11B, BHLHB5, *Tcerg1l, Ldb2, and Tox*, was no longer increased in layer 6 neurons in *Tle4*$^{-/-}$*; Fezf2-EnR* mice (Figure 7a, c-f and Supplemental Figure 3). However, expression of corticothalamic neuron genes, including ZFPM2 and FOXP2, and the subplate gene *Ctgf*, was not restored (Supplemental Figures 3 and 7). These results show that FEZF2 and TLE4 function together to prevent the high-level expression of subcerebral neuronal genes in corticothalamic neurons. They also suggest that, besides serving as a transcriptional co-repressor for FEZF2, TLE4 has additional functions in regulating the molecular differentiation of corticothalamic neurons.

We next compared the dendritic morphology and function of corticothalamic neurons in *Tle4*$^{-/-}$*; Fezf2-EnR* mice to *Tle4*$^{+/+}$ mice (Figure 6). Sholl analysis revealed that *Fezf2-EnR* rescued the decreased dendritic

branching ($p = 0.96$) and length ($p = 0.42$) observed in *Tle4*$^{-/-}$ corticothalamic neurons (Figure 6c). The changes in spine density ($p = 0.88$), spine head diameter ($p = 0.98$), and spine length ($p = 0.99$) were also reversed (Figure 6d). Patch clamp experiments showed that the *Fezf2-EnR* allele normalized the increased neuronal excitability associated with *Tle4*$^{-/-}$ neurons (Figure 6e). Corticothalamic neurons in *Tle4*$^{-/-}$*; Fezf2-EnR* and wild-type mice showed similar membrane resistance ($p = 0.53$), capacitance ($p = 0.87$) (Figure 6g), and mEPSC amplitude cumulative distribution and frequency (Figure 6h).

Taken together, these data suggest that FEZF2 and TLE4 together regulate the morphological and functional differentiation of corticothalamic projection neurons.

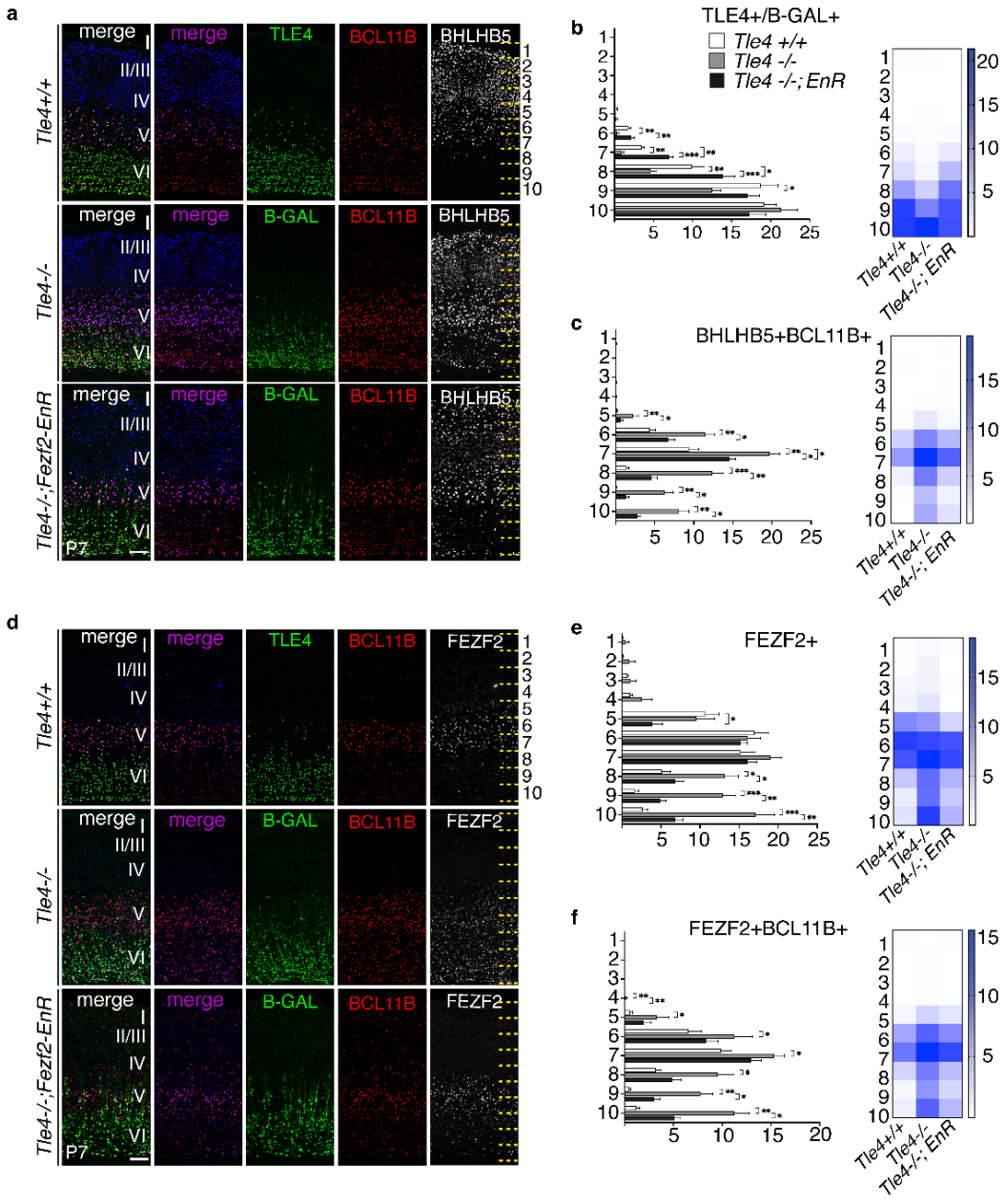

Figure 7. FEZF2-EnR represses the increased expression of subcerebral neuronal genes in the corticothalamic neurons in the *Tle4*$^{-/-}$ mice.
a. Immunostaining of TLE4 or B-GAL, BCL11B and BHLHB5 in the cortices of P7 *Tle4*$^{+/+}$, *Tle4*$^{-/-}$ and *Tle4*$^{-/-}$; *Fezf2-EnR* mice. **b**. Quantifications of TLE4^{+} cells in the *Tle4*$^{+/+}$ cortices and the B-GAL^{+} cells in *Tle4*$^{-/-}$ and *Tle4*$^{-/-}$; *Fezf2-EnR* cortices. **c**. Quantifications of the numbers of BCL11B^{+}BHLHB5^{+} cells. **d.** Immunostaining of TLE4, B-GAL, BCL11B and FEZF2 in the cortices of P7 *Tle4*$^{+/+}$, *Tle4*$^{-/-}$ and *Tle4*$^{-/-}$; *Fezf2-EnR* mice. **e**. Quantifications of the FEZF2^{+} cells by bin. **f**. Quantifications of

the numbers of $FEZF2^{+}BCL11B^{+}$ cells. n=3 brains per genotype, 3 sections per brain. Quantifications of $marker^{+}$ cells per 10,000 μm^2 in each bin. Heatmaps show the mean numbers of cells per 10,000 um^2 for each bin. In all graphs, error bars represent ± SEM. Statistical significance was determined using one-way ANOVA followed by post hoc Tukey's t-test (*$p<0.05$, **$p<0.01$, ***$p<0.001$).

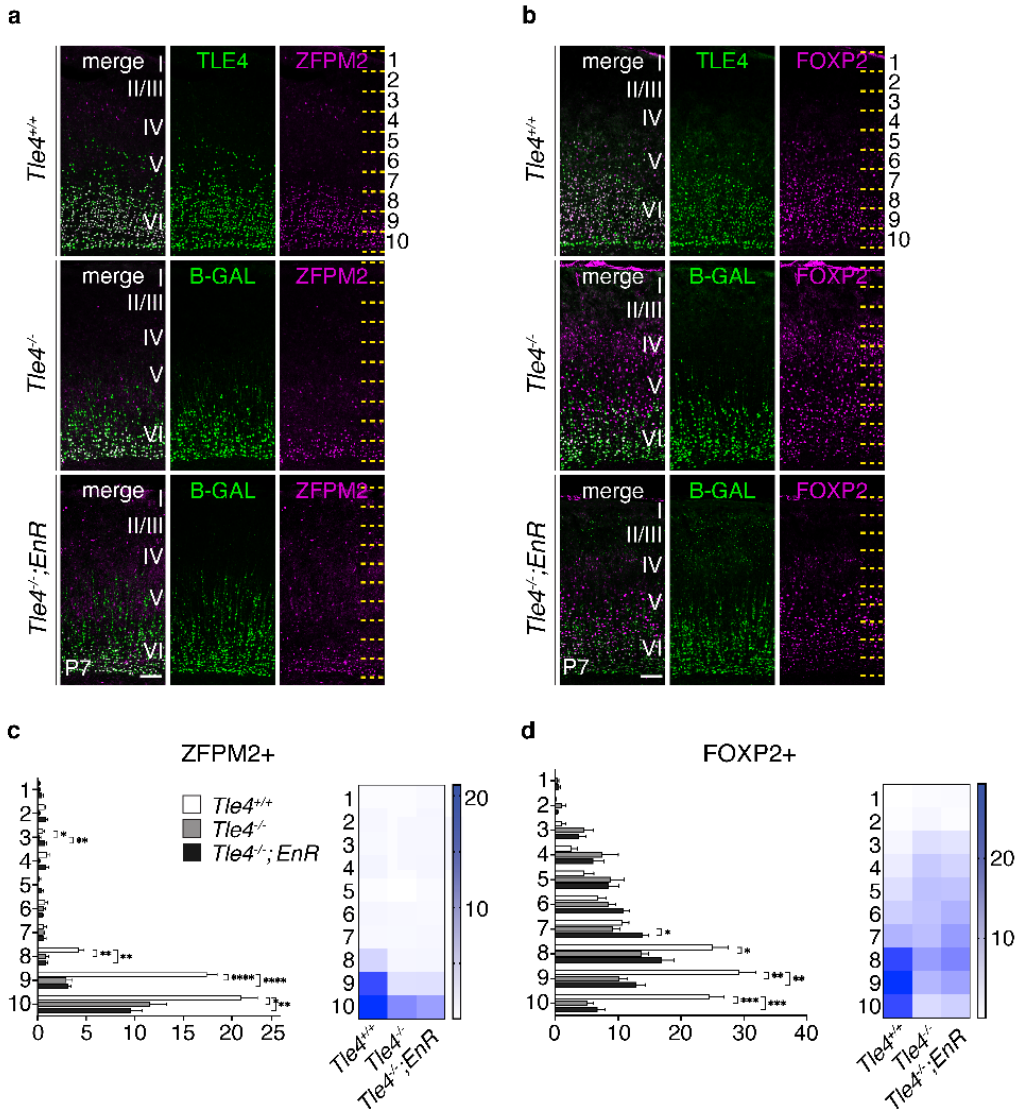

Figure S7. Reduced expression of layer 6 neuronal markers ZFPM2 and FOXP2 in the *Tle4*$^{-/-}$ mice were not rescued by the *Fezf2-EnR* allele.
a. Immunostaining for TLE4, B-GAL, and ZFPM2 in the cortices of P7 *Tle4*$^{+/+}$, *Tle4*$^{-/-}$ and *Tle4*$^{-/-}$; *Fezf2-EnR* mice. **b**. Immunostaining for TLE4, B-GAL and FOXP2. **c**. Quantifications of the ZFPM2^{+} cells by bin. **d**. Quantifications of the FOXP2^{+} cells by bin. n=3 brains per genotype, 3 sections per brain. Quantifications of marker^{+} cells per 10,000 μm^{2} in each bin. Heatmaps show the mean numbers of cells per 10,000 um^{2} for each bin. In all graphs, error bars represent ± SEM. Statistical significance was determined using one-way ANOVA followed by post hoc Tukey's t-test (*p<0.05, **p<0.01, ***p<0.001).

Discussion

Deciphering the molecular logic for establishing neuronal subtype identities in the developing cerebral cortex is fundamental to understanding how neuronal diversity is established in the mammalian brain. In this study we examined the molecular control of two broad classes of cortical projection neurons - the corticothalamic and the subcerebral projection neurons - by focusing on the function of FEFZ2.

Prior studies demonstrated that FEFZ2 is a master regulator for CSNs, a subpopulation of subcerebral neurons. In *Fezf2*$^{-/-}$ mice, subcerebral neurons were absent, and instead the mutant layer 5b neurons demonstrated the molecular features and axonal projection patterns of corticothalamic or corticocortical neuron subtypes (Chen et al., 2005; Chen et al., 2008; Chen J et al., 2005). Complementing these studies, ectopic expression of *Fezf2* in late cortical progenitors or upper-layer neurons, or in the progenitors of the lateral ganglionic eminence, led to the differentiation of neurons with gene expression and axon projections associated with corticothalamic or subcerebral neurons(Lodato et al., 2014; Chen et al., 2008; Chen J et al., 2005; Molyneaux et al., 2005; Rouaux et al., 2010; Rouaux et al., 2013; De la Rossa et al., 2013), suggesting that FEZF2 functions as a selector gene for subcerebral neurons. To test this, Lodato *et al.* (2014) performed gene expression analyses of cortical progenitors and neurons that over-expressed FEZF2, and ChIP-seq analysis of neurospheres that over-expressed FEZF2-

FLAG. Results from these experiments led the authors to conclude that FEZF2 functions as both a transcriptional activator and a repressor. They suggested that FEZF2 directly induces CSN glutamatergic identity by activating expression of genes including *Vglut1* (*Slc17a7*), and that it inhibits a GABAergic fate by repressing the transcription of genes such as *Gad1* (Lodato et al., 2014). They further reported that FEZF2 directly activates CSN-specific genes by binding to their proximal promoters and represses genes expressed in corticocortical projection neurons (Lodato et al., 2014).

Here we directly tested whether FEZF2 functions as a transcriptional activator, a repressor, or both, by comparing the activities of full-length FEZF2, FEZF2-EnR and FEZF2-VP16 chimeric proteins using two different assays. Results from both over-expression and rescue experiments showed that FEZF2-EnR recapitulated the activity of full-length FEZF2 protein, while the FEZF2-VP16 was less relevant in our assays. Thus, in contrast to prior work, our studies demonstrate that FEZF2 functions primarily as a transcriptional repressor, in context of the formation of corticospinal tract and neuronal identity. It is not clear why our results differ so markedly from those of Lodato *et al.* (2014), although it seems possible that ChIP-seq experiments may have overestimated the binding sites for FEZF2 in normal cortical neurons (Jain et al., 2015; Teytelman et al., 2013).

FEZF2 is required for establishing the molecular identity and axonal projections of both subcerebral and corticothalamic neurons. In the absence of *Fezf2*, subcerebral neurons exhibit molecular features and axonal projection patterns associated with corticothalamic or corticocortical neuron subtypes (Chen et al., 2005; Chen et al., 2008; Chen J et al., 2005). Previous reports (Diao et al., 2018; Komuta et al., 2007), and our current study show that in *Fezf2*$^{-/-}$ mice, corticothalamic neurons also exhibit defects in gene expression and axonal projections. We found that *Fezf2 cko* corticothalamic neurons showed increased expression of certain subcerebral neuronal genes such as BCL11B and the truncated FEZF2, indicating that corticothalamic neurons partially assume the molecular identity of subcerebral neurons in the absence of *Fezf2* function. Together these results suggest that FEZF2 inhibits the expression of distinct and specific target genes in subcerebral neurons and in corticothalamic neurons, and by doing so FEZF2 prevents each class of neurons from adopting an alternate neuronal subtype identity. Consistent with this, the *Fezf2-EnR* allele rescued the molecular identities and axonal projections of both the subcerebral and corticothalamic subtypes in *Fezf2*$^{-/-}$ mice.

How does FEZF2 function as a transcriptional repressor? One possibility is that FEZF2 binds to an enhancer or promoter sequence and physically prevents the binding of a transcriptional activator. Another possibility is that the binding of FEZF2 to an enhancer or promoter recruits

additional transcriptional co-repressor(s) and together they actively repress gene expression. In *Nex-Cre; Fezf2*$^{Flox/-l}$ mice, a truncated FEZF2 protein consisting of just the DNA binding domain was expressed, yet in these mice subcerebral and corticothalamic neurons and their axons showed similar defects as in *Fezf2*$^{-/-}$ null mutant mice (Figure 1 and Supplemental Figure 1). This result indicates that the N-terminal half of the FEZF2 protein is essential for its transcriptional repressor function, likely by recruiting transcriptional co-repressors, and that FEZF2 is unlikely to repress gene expression simply by blocking the binding of a transcriptional activator.

Indeed, FEZF2 contains an EH1 motif, which can recruit TLE family transcription co-repressors. The co-expression of FEZF2 and TLE4 in corticothalamic neurons suggests that TLE4 may be one of its co-repressors. Similar to *Fezf2*$^{-/-}$ mice, corticothalamic neurons in *Tle4*$^{-/-}$ mice showed increased expression of genes associated with subcerebral neurons, indicating that TLE4 is involved in refining the molecular identity of corticothalamic neurons by preventing high level expression of some subcerebral neuronal genes. We found that the *FEZF2-EnR* allele, which does not depend on TLE family transcription co-repressors for its function, prevented the high expression levels of subcerebral neuronal genes and restored the functional properties of corticothalamic neurons in *Tle4*$^{-/-}$ mice. These results support the conclusion that FEZF2 and TLE4 together repress the expression of FEZF2, BCL11B and BHLHB5 in corticothalamic neurons.

However, the reduced expression of corticothalamic neuronal genes such as FOG2 and FOXP2 in *Tle4*$^{-/-}$ mice was not rescued by the *Fezf2-EnR* allele. Furthermore, although corticothalamic axons were missing in *Fezf2*$^{-/-}$ mice, they were present in *Tle4*$^{-/-}$ mice. Thus, although FEZF2 and TLE4 together refine the molecular differentiation and function of corticothalamic neurons, each plays additional independent roles. The identity of possible co-repressor(s) for FEZF2 in subcerebral neurons remains unknown.

Recent progress and our current study show that the subtype identity of a cortical projection neuron is specified in the postmitotic stage. Multiple transcription factors, including *Tbr1* (McKenna et al., 2011; Han et al., 2011), *Sox5* (Kwan et al., 2008; Lai et al., 2008), *Fezf2* (Chen et al., 2005; Chen et al., 2008; Chen J et al., 2005) , and the chromatin remodeling protein *Satb2* (Alcamo et al., 2008; McKenna et al., 2015), are essential for specifying cortical projection neuron subtype identities . A common phenotype of mice with mutations in these genes is that the affected neuronal subtypes exhibit gene expression profiles and axonal projection patterns associated with alternate neuronal subtypes. This suggests that TBR1, SOX5, and SATB2 likely also function as selective repressors in their respective neuronal subtypes to inhibit expression of genes associated with alternate identities. In the future, it will be important to test whether these proteins act as transcriptional repressors, activators, or both, in the context of cortical projection neuron subtype specification. Another common feature shared by

the *Tbr1*, *Sox5*, and *Satb2* genes is that all are expressed in postmitotic neurons. Although *Fezf2* is expressed by both cortical RGCs and deep-layer neurons, our results indicate that it is required in postmitotic neurons for specifying cortical neuron subtype identities. These results suggest that projection neuron subtype-specific features are established through repressing genes associated with alternate subtype identities during postmitotic neuronal differentiation.

Although different subtypes of cortical projection neurons have distinct morphologies, axonal projection patterns, and molecular profiles, they share a common cortical regional identity and use glutamate as an excitatory neurotransmitter. A fundamental question in brain development is whether a single genetic program specifies both the pan-cortical excitatory neuron identity and the subtype-specific identity of a cortical projection neuron, or these features are specified by distinct genetic programs. Projection neuron subtype identities are mis-specified in *Fezf2*$^{-/-}$, *Tbr1*$^{-/-}$, *Sox5*$^{-/-}$ and *Satb2*$^{-/-}$ mice, but mutant cortical neurons maintain their glutamatergic identity and fail to acquire molecular features associated with GABAergic neurons. Thus, the subtype identity genes are not required for the adoption of a pan-cortical glutamatergic identity.

A different set of transcription factors, expressed in the RGCs and/or intermediate progenitors, including *Pax6*, *Tlx*, *Dmrt5*, *Dmrt3*, *Emx2*, *Ngn1*,

and *Ngn2*, are essential for establishing the regional and glutamatergic identities of cortical projection neurons (Konno et al., 2019; Desmaris et al., 2018; Kroll et al., 2005; Schuurmans et al., 2004). Based on our results and previous studies, we propose that the common vs. unique characteristics of cortical projection neuron subtypes are specified sequentially during development. At early stages of corticogenesis, transcription factors expressed in cortical RGCs and/or intermediate progenitors (including *Pax6*, *Tlx*, *Dmrt5*, *Dmrt3*, *Emx2*, *Ngn1*, and *Ngn2*) act in parallel pathways to ensure the generation of cortical glutamatergic projection neurons and prevent the production of ventral GABAergic neurons (Konno et al., 2019; Desmaris et al., 2018; Kroll et al., 2005; Schuurmans et al., 2004). As postmitotic cortical neurons begin to migrate and differentiate, genes such as *Fezf2*, *Tbr1*, *Sox5*, and *Satb2* repress the expression of genes associated with alternate neuronal subtype identities to establish specific subtype-specific identities. In the future, it will be necessary to rigorously test whether the proteins encoded by these genes function as transcriptional repressors or activators during development, and to determine how the expression of neuronal subtype identity genes is initially activated. Answers to these questions will be invaluable for designing novel and efficient strategies for using directed differentiation or trans-differentiation methods to repair damaged brain circuits in disease and injury.

Materials and Methods

Animals

Experiments were performed according to protocols approved by the Institutional Animal Care and Use Committee at University of California at Santa Cruz and at University of Arizona College of Medicine Phoenix, and were performed in accordance with institutional and federal guidelines. Experiments performed at Fudan University were in accordance with institutional guidelines.

We generated the *Tle4/Grg4* mutant allele by inserting a *LacZ-ires-Plap* cassette in the intron after the exon 4 of the *Tle4* gene, using the targeted gene trap strategy (Friedel et al., 2005). Southern hybridization was performed to screen the E14a ES cell clones and identify the correct targeting.

The bacterial artificial chromosome (BAC) clone RP23-141E17 was modified by inserting the cDNA encoding the ENGRAILED transcriptional repressor domain (EnR) fused with the DNA binding domain of FEZF2, followed by the SV40 polyadenylate site (*Fezf2-EnR*), at the start codon of the mouse *Fezf2* gene. The BAC DNA was purified and sequenced, and used for injection to generate the *Fezf2-EnR* transgenic mouse line.

The day of the vaginal plug detection was designated as E0.5. The day of birth was designated as P0. The genders of the embryonic and early postnatal mice were not determined.

PLAP staining

Human placental alkaline phosphatase (PLAP) staining was performed as described previously (Chen et al., 2005).

Immunohistochemistry

4% paraformaldehyde was delivered to mice via trans-cardiac perfusion. Brains were post-fixed in 4% paraformaldehyde, 0.1% saponin, and PBS for 24 hours at 4°C, followed by cryoprotection in 30% sucrose in PBS. Immunohistochemistry was performed using standard protocols. Briefly, twenty-five-μm-thick brain sections were permeabilized with 0.03% Triton X-100 in PBS for 30 min. Slides were then immersed in citrate buffer (10mM citric acid monohydrate, 0.05% Tween-20, pH 6.0), brought to a boil in a microwave and rested for 1 hour at RT. Slides were then incubated in a blocking buffer (5% donkey serum, 0.03% Triton X-100 in PBS) for 30 minutes. Blocking buffer was removed, and the sections were incubated with primary antibodies (diluted in the blocking buffer) for 24 hours at 4°C. The following primary antibodies were used in this study: GFP (Chicken, Aves Labs GFP-1020), BCL11B (Rat, Abcam ab18465), TBR1 (Rabbit, Abcam

ab31940), SOX5 (Rabbit, Abcam ab94396), FEZF2 (Rabbit, IBL F441), TLE4 (Mouse, Santa Cruz Biotechnology sc-365406), FOXP2 (Rabbit, Abcam ab16046) , ZFPM2 (Rabbit, Santa Cruz Biotechnology), B-GAL (Chicken, Abcam ab9361), activated caspase 3 (Rabbit, Cell Signaling Technology #9661), BHLHB5 (Goat, Santa Cruz Biotechnology sc-6045), SATB2 (Rabbit, Abcam ab34735), FOSL2 (Rabbit, Sigma HPA004817) , and GAPDH (Covance, MMS-580S), The sections were washed in PBS, and incubated with secondary antibodies conjugated to Alexa 488, Alexa 546, or Alexa 647 for 2 hours at room temperature. Secondary antibodies were from Jackson ImmunoResearch and Invitrogen. Finally, the sections were counterstained with DAPI for 5min before being mounted in Fluoromount-G.

In situ hybridization

In situ hybridization was performed using a previously published protocol[19]. In brief, digoxigenin-labeled probes used in this study were made from cDNAs amplified by PCR using the following primers:

Gene	Forward Primer 5' → 3'	Reverse Primer 5' → 3'
Tcerg1l	CTCTCCCCACTGTGGTATTAGC	CAGAACTATTTCCCCTCGTGAC
Ldb2	CACCTGATTACGCTGTCCATAG	AAGTTCAACACACGAGGGAGAT
Tox	GCTTTGTTCTTTCGTGATACCC	CGGGTTGAAGAGTAAATCCTTG
Ctgf	AAATCGCCAAGCCTGTCAAG	GGCACTGTGCGCTAATGAAC
Cryab	CTCAGCCCTGCCTGTGTT	ATCTGGGCCAGCCCTTAG

Amplified DNA fragments were ligated into pGEM-T Easy (Promega) plasmids, transformed into competent *E. coli* cells, and plated overnight on LB+Agar+Ampicillin plates. Colonies were picked, grown overnight in 3 mL LB+Ampicillin, and purified via miniprep kits (Sigma-Aldrich). Purified plasmids were sequenced to ensure sequence fidelity, and to determine insert orientation. Plasmids were then linearized with restriction enzymes from New England Biotech, and *in vitro* transcription reactions were performed with either T7 (NEB) or Sp6 (Promega) RNA polymerases, depending on insert orientation, in the presence of DIG-labeled nucleotides (Sigma-Aldrich). Tissue was prepared as previously described by Guo et al. (2013), and treated with DIG-labeled probes overnight at 65° C. Slides were developed with NBT/BCIP stock solution (Sigma-Aldrich)

EdU labeling

Timed pregnant *Tle4*$^{+/-}$ mice were injected with a single dose of EdU (50mg/kg body weight; Thermo Fisher Scientific, E10187) at E12.5 or E13.5. Brains were collected at P7. EdU was detected via a click-chemistry reaction containing the following reagents per 1 ml of reaction: 950ul 100mM Tris PH 7.4, 40ul 100 mM CuSO4, 10ul 200 mg/mL sodium ascorbate, and 1ul azide 488 or 555. *Tle4*$^{-/-}$ and littermate *Tle4*$^{+/-}$ control mice were analyzed.

Anterograde tracing using AAV

0.25 µl AAV2-CMV-mCherry virus (Vector Biosystems Inc.) were injected into the M1, S1 or V1 of *Tle4*$^{-/-}$ and littermate control *Tle4*$^{+/-}$ or *Tle4*$^{+/+}$ mice at P21. The brains were collected at P35 and sectioned at 50-µm thickness.

Retrograde tracing

Retrograde tracing was performed using Alexa Fluor 555-conjugated cholera toxin subunit β (CTB) injections. 8 mg/ml CTB in PBS was used for all injections, and CTB solution was injected through a pulled glass pipet attached to a Picospritzer III (Parker). P4 mice were anesthetized, the pyramidal decussation was identified visually, and 1 µl CTB was injected. 0.2 to 0.5 µl CTB was injected into S1 in anesthetized P4 mice and injection sites were confirmed after brain collection at P7. Corticothalamic neurons were labeled by CTB injection (0.2 µl) into the thalamus at P21 (coordinates: A/P -1.3 mm, M/L 3 mm, Z 3.15 mm) and injection sites were confirmed after brain collection at P28.

Cloning of the *pCAG-Fezf2*, *pCAG-Fezf2-EnR, and the pCAG-Fezf2-VP16* expression plasmids

The cloning of *pCAG-Fezf2* plasmid was reported previously (Chen et al., 2005). The EnR and VP16 plasmids were obtained from Dr. Thomas Jessell (Columbia University). The cDNA for DNA binding domains of FEZF2

was amplified using primers 5'-GATCGAATTCTCAGCTCTGAACTGTCCTGGCTAGGTC-3' and 5'-GATCGGATCCGCCGCCGCCATGGAGCCCCGGCCTGCTGCGTTAGAGGC-3'.

The cDNA for the EnR domain was amplified using primers 5'-GATCGATATCAAGCTTGGGCTGCATAGATCCCAG-3' and 5'-GATCGGATCCGCCGCCACCATGGAGTTCCGCGATGCCCTGGAGGATCGC-3'. The cDNA for VP16 domain was amplified using primers 5'-GATCGGATCCGCCGCCACCATGGCCCCCCCCGACCGATGTCAGCCT-3' and 5'-GATCGATATCCCCACCGTACTCGTCAATTCCAA-3'. The amplified DNA fragments were ligated into *pCAG* vector, using NotI and XhoI restriction sites. Sanger DNA sequencing was performed to ensure no mutation was generated during the cloning.

In utero electroporation

In utero electroporation experiment was performed according to a published protocol (Chen et al., 2005). *In utero electroporation* (IUE) of wild-type CD-1 embryos was performed at E15.5. Plasmids *pCAG-Fezf2*, *pCAG-Fezf2-EnR*, or *pCAG-Fezf2-VP16* were mixed with *pCAG-EGFP* (Addgene #11150) (final concentration of 1-2 μg/μl at a molecular ratio of 3:1, 0.5μl each embryo) and 0.05% Fast Green (Sigma), and injected into the lateral ventricle of embryos using a beveled pulled glass micropipette. The control brains

were electroporated with *pCAG-EGFP* plasmids alone. Five electrical pulses (duration: 50 ms) were applied at 35V across the uterine wall with a 950 ms interval between pulses. Electroporation was performed using a pair of 7-mm platinum electrodes (BTX, Tweezertrode 45-0488, Harvard Apparatus) connected to an electroporator (BTX, ECM830). The electroporated brains were collected at P5.

Image acquisition and analysis

Images for quantitative analyses were acquired with a Zeiss 880 confocal microscope. Laser power and gain were adjusted until <1% of pixels were saturated. Cell counting was performed on single z-slices with FIJI. Z-slices were divided into 500 μm or 250 um wide regions and split into equally sized bins. Individual channels were adjusted with auto threshold “Moments,” or a manual threshold was applied to discern BCL11B high versus low expressing cells. The dilate, erode, and watershed functions were sequentially used before particles were analyzed with a circularity of 0.3-1.0 and size exclusion of >1μm. Brightfield images were acquired with a Zeiss AxioImager Z2 widefield microscope with a Zeiss AxioCam 506 (color) camera.

Statistical analysis was performed using GraphPad Prism 5.0, or R. Only single Z-slice confocal images were used in cell quantifications. For each brain, the number of marker$^+$ cells in the cortex were quantified in a 500-

or 250-μm-wide region from 3 sections each for S1, M1 and V1 areas. Care was taken to match the anterior-posterior, medial-lateral positions for the chosen areas between the mutant and control genotypes. For each genotype and each age, 3 different brains were analyzed. Data are shown as mean ± SEM and statistical significance for multiple comparisons was determined using the ordinary one-way ANOVA test followed by Tukey's multiple comparisons test. Statistical significance for single comparisons was determined using the unpaired t-test. Significance was set as * for $p < 0.05$, ** for $p < 0.01$, *** $p < 0.001$ for and ****$p<0.0001$ all significance tests.

RNA-seq analysis of *Tle4*$^{-/-}$ and *Fezf2*$^{Plap/Plap}$ cortices at P0

Cortices were dissected from P0 *Tle4*$^{-/-}$ and littermate control *Tle4*$^{+/+}$ mice, P0 *Fezf2*$^{Plap/Plap}$ and littermate *Fezf2*$^{+/+}$ mice (n=3 for each genotype). Total RNA from each pair of cortical hemisphere was isolated using the RNAesay kit (Qiagen) and used to prepare RNA-seq libraries (Illumina RNA Truseq Library Prep protocol). Libraries were paired-end (50 nucleotides per end) sequenced on the Illumina Hiseq2000 platform. The sequences were processed and analyzed for differential expression as previously described (Betancourt et al., 2013). The RNA-seq data for the *Fezf2*$^{Plap/Plap}$ and control cortices, and for the *Tle4*$^{-/-}$ and control cortices can be accessed using GEOXXX and GSE142269.

Electrophysiology and neuronal morphology

Whole cell recording was conducted in the primary somatosensory cortex (V1). To label layer 6 corticothalamic neurons, 50nl of retrobeads (Lumafluor) were injected into the POM nucleus unilaterally at least 24h prior to recording. 350-μm slices were made after a block cut of the posterior brain with a 45° angle to the mid-sagittal plane. Slices were cut in ice-cold ACSF (containing 126 mM NaCl, 2.5 mM KCl, 26 mM $NaHCO_3$, 2 mM $CaCl_2$, 1 mM $MgCl_2$, 1.25 mM NaH_2PO_4, and 10 mM glucose saturated with 95% O_2 and 5% CO_2). Slices were incubated at 32°C for 30 min before being transferred to the recording chamber. $Beads^+$ neurons with soma in layer 6 were identified under a 60X objective (NA = 0.9). Only neurons with their soma at least 50 μm below the slice surface were targeted for whole cell recordings. The internal electrode solution contains: 130 mM K-gluconate, 10 mM HEPES, 4 mM KCl, 0.3 mM GTP-Na, 4 mM ATP-Mg, 2 mM NaCl,1 mM EGTA and 14 mM phosphocreatine (pH 7.2, 295-300 mOsm). 0.15% (W/V) biocytin was added when neuron morphology data were desired.

Neuronal signals were amplified using a MultiClamp 700B amplifier (Molecular Devices, Forster City, CA), low-pass filtered at 1 kHz (current) or 10 kHz (voltage signals), and digitized at 20 kHz using a Digidata 1440A interface and pClamp 10.6 (Molecular Devices). mEPSCs were measured with D-AP5 (50 μM, Tocris) and tetrodotoxin (TTX, 1μM, Tocris) included in the ACSF. To measure mIPSCs, TTX (1 μM) and CNQX (10 μM) were

included and a symmetrical [Cl-] electrode internal solution (containing: 125 mM KCl, 2.8 mM NaCl, 2 mM $MgCl_2$, 2 mM Mg^{2+}-ATP, 0.3 mM Na_3GTP, 10 mM HEPES, 1 mM EGTA and 10 mM phosphocreatine, pH 7.25, ~300 mOsm) was used. In experiments where neuronal excitability was measured, a series of current steps (-100 to 500pA in 50 pA increment) were injected, and numbers of AP firing were manually quantified.

To reconstruct neuronal morphologies, slices were fixed in 4% PFA overnight, followed by incubation with avidin-Alexa 488 (Invitrogen) for 24 h in PBS containing 0.2% Triton X-100. Slices were washed and mounted on slides with a 350-μm spacer to prevent crushing the tissue. Neuronal dendritic arbors were acquired by collecting Z-stack images on a confocal microscope (Zeiss LSM 710). Maximal projection images were imported into FIJI/ImageJ, and neurite arborization and Sholl analysis (Sholl, 1953) were done using the Simple Neurite Tracer plugin. Due to the length of apical dendrites, dendrites were frequently cut off. Therefore, only basal dendrites were used for Sholl analysis. Morphometric features extracted included dendritic arbor, length, and number of intersections at various distances from soma. For dendritic spine analyses, Z-stacks of spines from the basal dendrites (100-450 μm away from soma) were collected with a 63x objectives (Plan-Apochromat, NA 1.4). 512×512 pixels with 4× digital zoom and 0.2 μm Z step size were used for Z-stack acquisition. Imaris software (V8.02, Bitplane, South Windsor, CT)

was used to measure spine head diameter, length, and density (Peng et al., 2016).

Chapter 3: Conclusions and Future Directions

In the previous chapter, I have presented and interpreted the results of experiments focused on understanding how *Fezf2* and *Tle4* function to specify and maintain corticothalamic projection neuron subtype in the mammalian cerebral cortex. More specifically, we have shown that in corticothalamic neurons, FEZF2 and TLE4 function together to co-regulate the molecular differentiation, dendritic morphology, and function of these neurons. In doing so, we have also generated three novel mouse lines, *Fezf2-flox*, *Fezf2-BAC-EnR* and *Tle4 KO*, which will be useful for future studies as well. Overall, this work has shed light onto the intricate pathways required for the proper generation and maintenance of layer 5 and 6 excitatory projection neurons.

Insight into the function of TLE4 in CThPNs

Despite the widely accepted fact that TLE4 is highly expressed in CThPNs, the role it plays in the generation, maintenance, or function of these neurons was completely unknown until now. Through the generation of the novel transgenic *Tle4* knockout mouse line, I was able to meticulously investigate the various roles that TLE4 may play in CThPNs. Through the results shown and discussed earlier, we now have a much deeper

understanding of the role TLE4 in this cell type. The striking similarities between the phenotypes of layer 6 neurons between the *Tle4* and *Fezf2* knockout mice then prompted us to investigate whether these two proteins interact to functionally regulate transcription, thus specifying neuronal subtype.

The results of this study have also begun to tease apart the mechanisms FEZF2 uses to specify specific corticofugal subtype identity within the developing cerebral cortex. Specifically, I show that TLE4 is highly expressed in postmitotic CThPNs and is required to specify the molecular characteristics of these neurons, and it does so through binding FEZF2 and repressing SCPN genes. The interaction of FEZF2 and TLE4 was also shown to regulate the electrophysiological properties of CThPNs. These results provide convincing evidence that the cooperative transcriptional repression of SCPN genes by FEZF2 and TLE4 in newborn postmitotic neurons is necessary for proper cortical development. CThPNs are important for the proper processing and integration of sensory information, and their dysfunction has been implicated in epilepsy (Mattson, 2003).

The gene *Tbr1* (T-box, Brain, 1) codes for a transcription factor that is also highly expressed in CThPNs. Among other defects, CThPNs are completely absent in the cortex upon the deletion of *Tbr1*. Thus, *Tbr1* is often considered to be the master regulator of CThPN development. Interestingly, when we performed ChIP-seq for the TBR1 protein in the mouse cortex, we

saw a large binding peak just upstream of the *Tle4* gene (Darbandi et al., 2018). Additionally, through bulk RNA sequencing of the cortices of *Tbr1 KO* mice, we saw a severe reduction of *Tle4* expression levels compared to control cortices (Darbandi et al., 2018). However, these two results were not discussed or interpreted in the manuscript, I have just noted these results from the data. I also performed immuno-staining for TLE4 protein in the *Tbr1 KO* cortex, which showed a very dramatic reduction in the number of TLE4 positive neurons, (unpublished). These data combine to suggest that *Tbr1* likely acts to promote *Tle4* expression in the transcriptional pathway of CThPN fate specification. Despite these clear preliminary results, this claim should be taken merely as a hypothesis, as it has yet to be adequately tested. I do, however, believe that testing and confirming this hypothesis will likely hold valuable information relevant to human health, as the proper function of CThPNs has been implicated in mental disorders as mentioned earlier.

Future implications in SCPN fate-specification by *Fezf2*

Previously, it was unknown whether *Fezf2* specified SCPN identity in RGCs or newly born postmitotic neurons. Through our innovative use of transgenic strategies is mice, we were able to reliably and thoroughly tease apart this fundamental question. I believe results such as these truly emphasize the necessity of the deep and focused research into the

transcriptional regulation mechanisms in specific cell subtypes. Many studies have made claims about the broad functions of transcription factors, but our results clearly show that a single transcription factor can play extremely different roles dependent upon the cell type they are expressed in. It will be important to not only understand which transcription factors function differently in alternate progenitor and neuronal subtypes, but to also actually decipher the mechanisms that the transcription factors utilize to tightly control target gene expression levels. Recently, *Fezf2* has been implicated in a wide variety of human disorders from the promotion of bladder cancer by regulating the NF-KB signaling pathway (Chen et al., 2018), to acting as a key regulator of autoimmunity in medullary thymic epithelial cells to eliminate T cells that respond to self-antigens (Takayanagi et al., 2015). Thus, working towards a complete understanding of *Fezf2* as a transcriptional regulator on a molecular level will prove invaluable across many disciplines.

Upon interpreting the results presented above, many new and exciting questions have been raised. I believe that in the future it will be necessary to carefully isolate specific cell subtypes with techniques such as fluorescently activated cell sorting (FACS) followed by mass spectrometry (MS), in order to perform in-depth analysis of proteins that interact with FEZF2 in specific cellular subtypes. With recent advances in the applications of mass spectrometry, it is becoming more and more feasible to perform proteomic analysis on very small numbers, or even single cells, such as in the case of

SCoPE-MS (Budnik et al., 2018). These advanced technologies are still very resource intensive, but as they become more accessible, they will be extraordinarily useful for protein analyses such as the one I have just mentioned. Understanding the proteins other than TLE4 that interact with FEZF2 will provide useful insight into the function of this transcription factor that has been repeatedly implicated as a key player in a wide variety of human disorders affecting different cell types. This will vastly broaden the scope of potential targets when designing therapeutics for diseases in which FEZF2 is implicated.

Once we have a better understanding of the protein structures formed with FEZF2, the next step will be to again isolate specific cell subtypes and perform chromatin immunoprecipitation followed by RNA sequencing (ChIP-seq) for FEZF2 and its interacting proteins. This will inform not only the genes FEZF2 binds and regulates, but also it will inform which region of the gene FEZF2 typically binds. Again, this type of knowledge will open up new avenues for the development of therapeutics for the devastating diseases in which FEZF2 is implicated. Sometime in the near future, as DNA modifying technologies such as CRISPR-Cas9 continue to be optimized, it will be possible to target and modify very specific regions within the human genome. Thus, the simultaneous investigation into various regulatory DNA sequences and the proteins that bind them, such as TLE4 and FEZF2, will be essential

for the continuous advancement of effective and individualized medical treatment options.

Implications in human health

One potential application of this work is in regenerative medicine. Currently, there is much hope and effort surrounding stem cell therapies for the treatment of degenerative diseases such as Alzheimer's, Parkinson's, and ALS**.** Understanding the mechanisms behind the generation and maintenance of the neuronal subtypes affected in these devastating diseases is fundamental to continually advance the efficacy of therapeutics aimed at these diseases. In order to effectively use stem cell replacement therapies, we must be able to efficiently and specifically generate distinct neuronal subtypes that are lost or damaged in these disorders. To do this, we must have a deep understanding of the molecular mechanisms underlying these fate decisions in order to generate neurons that are as similar to healthy endogenous neurons as possible. In this study, we show that upon *Tle4* deletion, corticothalamic neurons still project to the thalamus, but their electrophysiological properties are significantly affected. One interesting observation I noticed during my experiments, but never fully analyzed, was that *Tle4* mutant mice appeared to exhibit multiple behavioral abnormalities. For example, these mice would often be seen running in tight clockwise

circles and speed up when frightened. Also, it was noted that the *Tle4* knockout mice were more susceptible to audiogenic seizures than control mice. This is consistent with the findings that implicate defective corticothalamic neuron function in humans as a main contributor to epilepsy. This strongly exemplifies our need to continue to deeply investigate the molecular mechanisms underlying subtype specification and function. Despite the ability of CThPNs to reach the thalamus in *Tle4* mutant mice, their dysfunction may lead to abnormal behavioral phenotypes. Without careful and thorough analysis, the initial results of this study could have been extremely misleading, which could be catastrophic in the context of regenerative stem cell transplant therapies. This implicates the need for an extremely thorough understanding of the molecular mechanisms involved in the proper generation and function of cortical neuron subtypes. In conclusion, this dissertation has not only confronted and convincingly corrected multiple common misconceptions, but has also uncovered novel mechanisms involved in the transcriptional regulation of cortical neuron subtype specification.

Bibliography

Alcamo, E. A. et al. Satb2 regulates callosal projection neuron identity in the developing cerebral cortex. *Neuron* 57, 364-377 (2008).

Arlotta, P. et al. Neuronal subtype-specific genes that control corticospinal motor neuron development in vivo. *Neuron* 45, 207-221 (2005).

Balasubramanian M. et al. Case series: 2q33.1 microdeletion syndrome--further delineation of the phenotype. *J Med Genet 48*, 290-298. (2011).

Betancourt, J., Katzman, S. & Chen, B. Nuclear factor one b regulates neural stem cell differentiation and axonal projection of corticofugal neurons. *J Comp Neurol*, doi:10.1002/cne.23373 (2013).

Bizzotto S, Francis F. Morphological and functional aspects of progenitors perturbed in cortical malformations. *Front Cell Neurosci* 9,30 doi:10.3389/fncel.2015.00030 (2015).

Britanova, O. et al. Satb2 is a postmitotic determinant for upper-layer neuron specification in the neocortex. *Neuron* 57, 378-392 (2008).

Chen, B., Schaevitz, L. R. & McConnell, S. K. Fezl regulates the differentiation and axon targeting of layer 5 subcortical projection neurons in cerebral cortex. *Proc Natl Acad Sci U S A* 102, 17184-17189, doi:10.1073/pnas.0508732102 (2005).

Chen, B. et al. The *Fezf2*-Ctip2 genetic pathway regulates the fate choice of subcortical projection neurons in the developing cerebral cortex. *Proc Natl Acad Sci* U S A 105, 11382-11387 (2008).

Chen, G., Courey, A. Groucho/TLE family proteins and transcriptional repression, *Gene*, 249, 1–21-16, 10.1016/s0378-1119(00)00161-x (2000)

Chen, J. G., Rasin, M. R., Kwan, K. Y. & Sestan, N. Zfp312 is required for subcortical axonal projections and dendritic morphology of deep-layer pyramidal neurons of the cerebral cortex. *Proc Natl Acad Sci* U S A 102, 17792-17797 (2005).

Clare, A. J., Wicky, H. E., Empson, R. M. & Hughes, S. M. RNA-Sequencing Analysis Reveals a Regulatory Role for Transcription Factor *Fezf2* in the Mature Motor Cortex. *Front Mol Neurosci* 10, 283, doi:10.3389/fnmol.2017.00283 (2017).

Courey, AJ., Jia, S. Transcriptional repression: the long and short of it. *Genes Dev*. Nov 1;15(21):2786-96 (2001).

Fazel Darbandi, Siavash et al. “Neonatal Tbr1 Dosage Controls Cortical Layer 6 Connectivity.” *Neuron* vol. 100,4 831-845.e7 doi: 10.1016/j.neuron.2018.09.027 (2018).

De la Rossa, A. et al. In vivo reprogramming of circuit connectivity in postmitotic neocortical neurons. *Nat Neurosci* 16, 193-200, doi:10.1038/nn.3299 (2013).

Desmaris, E. et al. DMRT5, DMRT3, and EMX2 Cooperatively Repress Gsx2 at the Pallium-Subpallium Boundary to Maintain Cortical Identity in Dorsal Telencephalic Progenitors. *J Neurosci* 38, 9105-9121, doi:10.1523/JNEUROSCI.0375-18.2018 (2018).

Diao, Y. et al. Reciprocal Connections Between Cortex and Thalamus Contribute to Retinal Axon Targeting to Dorsal Lateral Geniculate Nucleus. *Cereb Cortex* 28, 1168-1182, doi:10.1093/cercor/bhx028 (2018).

Docker, D., Schubach, M., Menzel, M., Munz, M., Spaich, C., Biskup, S., and Bartholdi, D. Further delineation of the SATB2 phenotype. *Eur J Hum Genet, 22(8),* 1034-9. (2013).

Friedel, R. H. et al. Gene targeting using a promoterless gene trap vector ("targeted trapping") is an efficient method to mutate a large fraction of genes. *Proc Natl Acad Sci* U S A 102, 13188-13193 (2005).

Goebbels, S. et al. Genetic targeting of principal neurons in neocortex and hippocampus of NEX-Cre mice. *Genesis* 44, 611-621, doi:10.1002/dvg.20256 (2006).

Graham et al. SOX2 Functions to Maintain Neural Progenitor Identity. *Neuron* vol 39, 5, 749-765, doi: 10.1016/S0896-6273(03)00497-5. (2003).

Grosskreutz, Julian et al. “Widespread sensorimotor and frontal cortical atrophy in Amyotrophic Lateral Sclerosis.” *BMC neurology* vol. 6 17. 25, doi:10.1186/1471-2377-6-17 (2006).

Guo, C. et al. *Fezf2* expression identifies a multipotent progenitor for neocortical

projection neurons, astrocytes, and oligodendrocytes. *Neuron* 80, 1167-1174, doi:10.1016/j.neuron.2013.09.037 (2013).

Habert, H. et al. Brain perfusion imaging in amyotrophic lateral sclerosis: Extent of cortical changes according to the severity and topography of motor impairment, *Amyotrophic Lateral Sclerosis*, 8:1, 9-15, 10.1080/14660820601048815, (2007).

Han, W. et al. TBR1 directly represses *Fezf2* to control the laminar origin and development of the corticospinal tract. *Proc Natl Acad Sci* U S A 108, 3041-3046, doi:10.1073/pnas.1016723108 (2011).

Hashimoto, H. et al. Expression of the zinc finger gene fez-like in zebrafish forebrain. *Mech Dev* 97, 191-195 (2000).

Hevner RF, Shi L, Justice N, Hsueh Y, Sheng M, Smiga S, Bulfone A, Goffinet AM, Campagnoni AT, Rubenstein JL. Tbr1 regulates differentiation of the preplate and layer 6. *Neuron*. 29(2):353-66. (2001).

Hobert, O. & Kratsios, P. Neuronal identity control by terminal selectors in worms, flies, and chordates. *Curr Opin Neurobiol* 56, 97-105, doi:10.1016/j.conb.2018.12.006 (2019).

Ishiuchi T., Misaki K., Yonemura S., Takeichi M., Tanoue T. Mammalian fat and dachsous cadherins regulate apical membrane organization in the embryonic cerebral cortex. *J. Cell Biol*. 185, 959–967. 10.1083/jcb.200811030 (2009).

Jimenez, G., Paroush, Z., and Ish-Horowicz, D.. Groucho acts as a corepressor for a subset of negative regulators, including Hairy and Engrailed. *Genes & Dev*. 11: 3072–3082 (1997).

Jain, D., Baldi, S., Zabel, A., Straub, T. & Becker, P. B. Active promoters give rise to false positive 'Phantom Peaks' in ChIP-seq experiments. *Nucleic Acids Res* 43, 6959-6968, doi:10.1093/nar/gkv637 (2015).

Kadowaki M., Nakamura S., Machon O., Krauss S., Radice G. L., Takeichi M. N-cadherin mediates cortical organization in the mouse brain. *Dev. Biol*. 304, 22–33. 10.1016/j.ydbio.2006.12.014 (2007).

Klug, A., Rhodes, D. Zinc Fingers: A Novel Protein Fold for Nucleic Acid Recognition. *Cold Spring Harb Symp Quant Biol* 1987 52: 473-482; (1987)

Komuta, Y., Hibi, M., Arai, T., Nakamura, S. & Kawano, H. Defects in reciprocal projections between the thalamus and cerebral cortex in the early development of Fezl-deficient mice. *J Comp Neurol* 503, 454-465 (2007).

Konno, D. et al. Dmrt factors determine the positional information of cerebral cortical progenitors via differential suppression of homeobox genes. *Development* 146, doi:10.1242/dev.174243 (2019).

Kriegstein, Arnold, and Arturo Alvarez-Buylla. “The glial nature of embryonic and adult neural stem cells.” *Annual review of neuroscience* 32 149-doi:10.1146/annurev.neuro.051508.135600 (2009).

Kroll, T. T. & O'Leary, D. D. Ventralized dorsal telencephalic progenitors in Pax6 mutant mice generate GABA interneurons of a lateral ganglionic eminence fate. *Proc Natl Acad* Sci U S A 102, 7374-7379, doi:10.1073/pnas.0500819102 (2005).

Kwan, K. Y. et al. SOX5 postmitotically regulates migration, postmigratory differentiation, and projections of subplate and deep-layer neocortical neurons. *Proc Natl Acad Sci* U S A 105, 16021-16026 (2008).

Leone, D. P., Srinivasan, K., Chen, B., Alcamo, E. & McConnell, S. K. The determination of projection neuron identity in the developing cerebral cortex. *Curr Opin Neurobiol* 18, 28-35, doi:10.1016/j.conb.2008.05.006 (2008).

Leone, D. P. et al. Satb2 Regulates the Differentiation of Both Callosal and Subcerebral Projection Neurons in the Developing Cerebral Cortex. *Cereb Cortex* 25, 3406-3419, doi:10.1093/cercor/bhu156 (2015).

Lai, T. et al. SOX5 controls the sequential generation of distinct corticofugal neuron subtypes. *Neuron* 57, 232-247, doi:10.1016/j.neuron.2007.12.023 (2008).

Landisman, C. E. & Connors, B. W. VPM and PoM nuclei of the rat somatosensory thalamus: intrinsic neuronal properties and corticothalamic feedback. *Cereb Cortex* 17, 2853-2865, doi:10.1093/cercor/bhm025 (2007).

Li, M., Arnosti, D. Long- and short-range transcriptional repressors induce distinct chromatin states on repressed genes.*Current biology :* 21,5 406-12. 10.1016/j.cub.2011.01.054. (2011).

Liu, Z., Karmarkar, V. Groucho/Tup1 family co-repressors in plant development. *Trends Plant Sci*, 1 3(3):137-44. doi: 10.1016/j.tplants.2007.12.005. (2008)

Lodato, S. et al. Gene co-regulation by *Fezf2* selects neurotransmitter identity and connectivity of corticospinal neurons. *Nat Neurosci* 17, 1046-1054, doi:10.1038/nn.3757 (2014).

Martynoga B., Drechsel D. and Guillemot F. Molecular control of neurogenesis: a view from the mammalian cerebral cortex. *Cold Spring Harb Perspect Biol.* 4, a008359. (2012)

Mattson, R., Overview: Idiopathic Generalized Epilepsies. *Epilepsia,* 44: 2-6. doi:10.1046/j.1528-1157.44.s.2.3.x (2003).

McKenna, W. L. et al. Tbr1 and *Fezf2* regulate alternate corticofugal neuronal identities during neocortical development. *J Neurosci* 31, 549-564, doi:10.1523/jneurosci.4131-10.2011 (2011).

McKenna, W. L. et al. Mutual regulation between Satb2 and *Fezf2* promotes subcerebral projection neuron identity in the developing cerebral cortex. *Proc Natl Acad* Sci U S A 112, 11702-11707, doi:10.1073/pnas.1504144112 (2015).

Mizutani K., Yoon K., Dang L., Tokunaga A. and Gaiano N. Differential Notch signalling distinguishes neural stem cells from intermediate progenitors. *Nature* 449, 351–355. (2007)

Molyneaux, B. J., Arlotta, P., Hirata, T., Hibi, M. & Macklis, J. D. Fezl is required for the birth and specification of corticospinal motor neurons. *Neuron* 47, 817-831 (2005).

Molyneaux, B. J., Arlotta, P., Menezes, J. R. & Macklis, J. D. Neuronal subtype specification in the cerebral cortex. *Nat Rev Neurosci* 8, 427-437 (2007).

Molyneaux, B. J. et al. DeCoN: genome-wide analysis of in vivo transcriptional dynamics during pyramidal neuron fate selection in neocortex. *Neuron* 85, 275-288, doi:10.1016/j.neuron.2014.12.024 (2015).

Muhr, J., Andersson, E., Persson, M., Jessell, T. M. & Ericson, J. Groucho-mediated transcriptional repression establishes progenitor cell pattern and neuronal fate in the ventral neural tube. *Cell* 104, 861-873 (2001).

Näär, M. et al., Transcriptional Coactivator Complexes, *Annual Review of Biochemistry* 70:1, 475-501. 10.1146/annurev.biochem.70.1.475 (2001).

Nievergall E., Lackmann M., Janes P. W. Eph-dependent cell-cell adhesion and segregation in development and cancer. *Cell. Mol. Life Sci*. 69, 1813–1842. 10.1007/s00018-011-0900-6 (2012).

Notwell J.H., Heavner W.E., Darbandi S.F., Katzman S., McKenna W.L., Ortiz-Londono C.F., Tastad D., Eckler M.J., Rubenstein J.L., McConnell S.K., Chen B., Bejerano G. TBR1 regulates autism risk genes in the developing neocortex. *Genome Research.* (8):1013-22. (2016).

O'Leary, D. D. & Koester, S. E. Development of projection neuron types, axon pathways, and patterned connections of the mammalian cortex. *Neuron* 10, 991-1006 (1993).

Pelvig, D.P., Pakkenberg, H., Stark, A.K., and Pakkenberg, B. (2007). Neocortical glial cell numbers in human brains. *Neurobiol Aging, 29(11),* 1754-1762.

Peng, Y. et al. The autism-associated MET receptor tyrosine kinase engages early neuronal growth mechanism and controls glutamatergic circuits development in the forebrain. *Mol Psychiatry* 21, 925-935, doi:10.1038/mp.2015.182 (2016).

Rakic, P. Guidance of neurons migrating to the fetal monkey neocortex. *Brain Res* 2, 471-476, doi:10.1016/0006-8993(71)90119-3 (1971).

Rakic, P. Mode of cell migration to the superficial layers of fetal monkey neocortex. *J. Comp. Neurol*., 145: 61-83. doi:10.1002/cne.901450105 (1972).

Rouaux, C. & Arlotta, P. *Fezf2* directs the differentiation of corticofugal neurons from striatal progenitors in vivo. *Nat Neurosci* 13, 1345-1347, doi:10.1038/nn.2658 (2010).

Rouaux, C. & Arlotta, P. Direct lineage reprogramming of post-mitotic callosal neurons into corticofugal neurons in vivo. *Nature cell biology* 15, 214-221, doi:10.1038/ncb2660 (2013).

Schmid M. T., Weinandy F., Wilsch-Bräuninger M., Huttner W. B., Cappello S., Götz M. The role of α-E-catenin in cerebral cortex development: radial glia specific effect on neuronal migration. *Front. Cell. Neurosci*. 8:215. 10.3389/fncel.2014.00215 (2014).

Schuurmans, C. et al. Sequential phases of cortical specification involve Neurogenin-dependent and -independent pathways. *Embo J* 23, 2892-2902 (2004).

Shim, S., Kwan, K. Y., Li, M., Lefebvre, V. & Sestan, N. Cis-regulatory control of corticospinal system development and evolution. *Nature* 486, 74-79, doi:10.1038/nature11094 (2012).

Sholl, D. A. Dendritic organization in the neurons of the visual and motor cortices of the cat. *J Anat* 87, 387-406 (1953).

Tantirigama, M. L. et al. *Fezf2* expression in layer 5 projection neurons of mature mouse motor cortex. *J Comp Neurol* 524, 829-845, doi:10.1002/cne.23875 (2016).

Tasic, B. et al. Shared and distinct transcriptomic cell types across neocortical areas. *Nature* 563, 72-78, doi:10.1038/s41586-018-0654-5 (2018).

Teytelman, L., Thurtle, D. M., Rine, J. & van Oudenaarden, A. Highly expressed loci are vulnerable to misleading ChIP localization of multiple unrelated proteins. *Proc Natl Acad* Sci U S A 110, 18602-18607, doi:10.1073/pnas.1316064110 (2013).

Tolkunova, E N et al. “Two distinct types of repression domain in engrailed: one interacts with the groucho corepressor and is preferentially active on integrated target genes.” *Molecular and cellular biology* vol. 18,5: 2804-14. doi:10.1128/mcb.18.5.2804 (1998).

Willsey, A. J., Sanders, S. J., Li, M., Dong, S., Tebbenkamp, A. T., Muhle, R. A., … State, M. W. Coexpression networks implicate human midfetal deep cortical projection neurons in the pathogenesis of autism. *Cell*, *155*(5), 997–1007. (2013).

Zhang, S., Li, J., Lea, R., Vleminckx, K. & Amaya, E. *Fezf2* promotes neuronal differentiation through localised activation of Wnt/beta-catenin signalling during forebrain development. *Development* 141, 4794-4805, doi:10.1242/dev.115691 (2014).